

This is an Open Access document downloaded from ORCA, Cardiff University's institutional repository: <https://orca.cardiff.ac.uk/id/eprint/158264/>

This is the author's version of a work that was submitted to / accepted for publication.

Citation for final published version:

Palmer, Paul I., Wainwright, Caroline M. , Dong, Bo, Maidment, Ross I., Wheeler, Kevin G., Gedney, Nicola, Hickman, Jonathan E., Madani, Nima, Folwell, Sonja S., Abdo, Gamal, Allan, Richard P., Black, Emily C. L., Feng, Liang, Gudoshava, Masilin, Haines, Keith, Huntingford, Chris, Kilavi, Mary, Lunt, Mark F., Shaaban, Ahmed and Turner, Andrew G. 2023. Drivers and impacts of Eastern African rainfall variability. Nature Reviews Earth & Environment 10.1038/s43017-023-00397-x

Publishers page: <http://dx.doi.org/10.1038/s43017-023-00397-x>

Please note:

Changes made as a result of publishing processes such as copy-editing, formatting and page numbers may not be reflected in this version. For the definitive version of this publication, please refer to the published source. You are advised to consult the publisher's version if you wish to cite this paper.

This version is being made available in accordance with publisher policies. See <http://orca.cf.ac.uk/policies.html> for usage policies. Copyright and moral rights for publications made available in ORCA are retained by the copyright holders.



# Physical drivers and multifarious impacts of Eastern African rainfall variations

Paul I. Palmer<sup>1,2†</sup>, Caroline M. Wainwright<sup>3</sup>, Bo Dong<sup>4,5</sup>, Ross I. Maidment<sup>4</sup>, Kevin G. Wheeler<sup>6</sup>, Nicola Gedney<sup>7</sup>, Jonathan E. Hickman<sup>8,9</sup>, Nima Madani<sup>10,11</sup>, Sonja S. Folwell<sup>12</sup>, Gamal Abdo<sup>13</sup>, Richard P. Allan<sup>4,5</sup>, Emily C. L. Black<sup>4</sup>, Liang Feng<sup>1,2</sup>, Masilin Gudoshava<sup>14</sup>, Keith Haines<sup>4,5</sup>, Chris Huntingford<sup>12</sup>, Mary Kilavi<sup>15</sup>, Mark F. Lunt<sup>1</sup>, Ahmed Shaaban<sup>16,17</sup> and Andrew G. Turner<sup>4</sup>

1) School of GeoSciences, University of Edinburgh, Edinburgh, UK;

2) National Centre for Earth Observation, University of Edinburgh, Edinburgh, UK;

3) Grantham Institute, Imperial College London, London, UK;

4) Department of Meteorology, University of Reading, Reading, UK;

5) National Centre for Earth Observation, University of Reading, UK

6) The Environmental Change Institute, University of Oxford, Oxford, UK;

7) Met Office Hadley Centre, Joint Centre for Hydrometeorological Research, Wallingford, UK;

8) Center for Climate Systems Research, Columbia Climate School, Columbia University, New York, NY, USA;

9) NASA Goddard Institute for Space Studies, New York, NY, USA;

10) UCLA Joint Institute for Regional Earth System Science and Engineering, CA, USA;

11) Jet Propulsion Laboratory, Pasadena, CA, USA;

12) UK Centre for Ecology and Hydrology, Wallingford, UK;

13) Department of Civil Engineering, University of Khartoum, Khartoum, Sudan;

14) IGAD Climate Prediction and Applications Centre, Nairobi, Kenya;

15) Kenya Meteorological Department, Nairobi, Kenya;

16) Department of Atmospheric and Environmental Sciences, University at Albany, State University of New York (SUNY), Albany, NY, USA;

17) Egyptian Meteorological Authority, Cairo, Egypt.

† email: paul.palmer@ed.ac.uk

## Abstract

Eastern Africa experiences extreme rainfall variations that have profound socio-economic impacts. In this Review, we synthesize understanding of observed changes in seasonal regional rainfall, its global to local forcings, the expected future changes and the associated environmental impacts. We focus on regions where annual bimodal rainfall is split between long rains (March-May) and short rains (October-December). Since the early 1980s, the long rains have got drier (-0.13—1.23 mm/season/decade) although some recovery is observed in 2018 and 2020. Meanwhile, the short rains have got wetter (1.27—2.58 mm/season/decade). These trends, overlaid by substantial year-to-year variations, impact the severity and frequency of extreme flooding and droughts, the stability of food and energy systems, the susceptibility to water-borne and vector-borne diseases and ecosystem stability. Climate model projections of rainfall changes vary but there is some consensus that a warming climate will increase rainfall over Eastern Africa. Climate models suggest that by 2030-2040 the short rains will deliver more rainfall than the long rains, which has implications for sustaining agricultural yields and triggering climate-related public health emergencies. Mitigating the impacts of future Eastern African climate requires continued investments in agriculture, clean water, medical and emergency infrastructures that are commensurate to the upcoming existential challenges.

## Key points [30 words or fewer]

- Rainfall across Eastern Africa is changing rapidly with future projections suggesting these changes will continue, driven by increasing atmospheric greenhouse gases and by greater natural variability of the climate system.
- Within the 2030-2040 timeframe, climate models suggest that the short rains will deliver more rainfall over Eastern Africa than the long rains, subject to caveats, that has traditionally supported agriculture.
- During the 2030-2040 period, climate models suggest a higher frequency and severity of droughts that are also associated with significant humanitarian and socio-economic impacts.
- Projected rainfall changes will lead to widespread changes in agricultural yields and accessibility to clean water that will further increase the risk of food and water insecurity across Eastern Africa.
- Future rainfall changes will result in multifarious and long-term costs to human health and wellbeing, and the urban and natural environments.
- Development of adaptation strategies to improve agricultural yields and access to clean water, and to prepare for vector-borne disease outbreaks, will help avoid an unprecedented-scale public health emergency.
- Targeted improvements to meteorological observing systems will help improve the quality of meteorological forecasts over Eastern Africa that enable early warning systems to deliver better actionable information to individual countries

## Introduction

Seasonal rainfall is integral to the 457 million people living across Eastern Africa, a region including Somalia, Burundi, Djibouti, Ethiopia, Eritrea, Kenya, Rwanda, South Sudan, Sudan, Tanzania and Uganda (**Box 1**). The number, duration and timing of these seasons varies across the region, driven principally by the movement of the intertropical convergence zone (ITCZ)<sup>1</sup>. For instance, the most northern and southern countries (northern Ethiopia, Eritrea, Sudan, South Sudan and southern Tanzania) experience a single summer wet season for their respective hemisphere. In contrast, countries between these latitudinal extremes (encompassing Kenya, Uganda, Somalia, Burundi, Rwanda and parts of northern Tanzania and southern Ethiopia) experience two wet seasons. These two wet seasons occur during boreal spring (typically March-May, MAM; the more intense long rains) and autumn (typically October-December, OND; the less intense short rains), although there are substantial regional variations in these timings. We focus mainly on countries that have annual bimodal rainfall.

This seasonal rainfall is vital to the health and economic prosperity of the region. For example, long rains support agricultural production and thus national food security. Rain-fed agriculture, in turn, has a substantial role in the economy of many Eastern African countries. Agriculture employs 67% of people in Ethiopia, 80% in Somalia, 54% in Kenya, 63% in Eritrea and 38% in Sudan (data taken from World Bank Open Data). Agriculture also represents a substantial contribution to the annual multi-billion-dollar export of goods such as sugar, tea, coffee, tobacco, nuts and seeds, cut flowers and vegetables (taken from the Observatory of Economic Complexity). Moreover, rainfall is pivotal to energy production, particularly given that

hydropower represents a substantial fraction of electricity generation in Eastern Africa<sup>2</sup>. Aquifer recharge from rainfall<sup>3,4</sup> also provides a sustainable reservoir of groundwater for potable water (and irrigation) during periods of drought<sup>3</sup>, demonstrating the importance of rainfall for water security, especially when looking to the future<sup>5</sup>.

Observed rainfall variability, particularly the disruption to the long and short rains, can therefore result in a wide range of humanitarian, economic and environmental impacts. For example, three anomalously low rain seasons over Somalia from April 2016 to December 2017 resulted in sustained and widespread drought conditions that led to significant losses of agricultural crops and livestock<sup>6</sup>. Consequently, more than six million people faced acute food shortages and malnutrition<sup>7</sup>, exacerbated by a shortage of potable water that led to disease outbreak. A similar situation is unfolding in 2022 (ref<sup>8,9</sup>), with poor rain seasons since late 2020. In stark contrast, consecutive anomalously high rain seasons over South Sudan since 2019 has led to prolonged flooding, affecting more than 800,000 people<sup>10</sup>. Recurrent flooding has damaged water treatment facilities, leaving millions without potable water, resulting in the outbreak of cholera and diseases spread by mosquitoes. Fields that typically support subsistence farming are submerged by floodwater, leading to a significant reduction in land to cultivate. This situation is exacerbated by conflict<sup>10</sup>. As such, there are concerns over widespread disruptions to clean sources of energy<sup>2</sup>, depletion of surface and groundwater reservoirs<sup>11</sup>, devastating flooding events<sup>12</sup>, and reductions in agricultural crop yields<sup>13</sup> and livestock productivity<sup>14</sup>. To help mitigate such impacts and inform future adaptation changes, it is therefore vital to fully understand all aspects of Eastern African rainfall impacts, particularly in light of continued changes arising from anthropogenic warming<sup>15</sup>.

In this Review, we synthesize the literature regarding observed rainfall variations over Eastern Africa, focused on regions with a bimodal rainfall season, and their physical drivers. We subsequently outline the economic, humanitarian and environmental impacts of such observed rainfall variability. Based on state-of-the-art climate model projections, we also describe the major climatological changes anticipated for Eastern Africa, and the associated likely future impacts. Finally, we identify key gaps in knowledge and how these can be addressed in future research.

## 2 Drivers of Eastern African rainfall

The timing and magnitude of the seasonal cycle of rainfall varies across Eastern Africa (**Fig. 1**). A single peaked seasonal cycle is evident over the majority of the Nile basin during June–August, whereas two distinct rainfall seasons (short rains and long rains) are observed over the Juba-Shabelle and northeast coast basins; some combination of the two occur over the Rift Valley basin and the Central-East coast basin.

There are substantial seasonal and interannual variations in rainfall totals (**Fig. 1**). For example, the standard deviation of rainfall over the Nile Basin during August (typically the wettest month) is 17 mm month<sup>-1</sup>, representing ~12% of the long-term August mean rainfall according to the GPCC dataset. Whereas across the Juba-Shabelle Basin, rainfall is considerably more variable. The standard deviation is 36 mm month<sup>-1</sup> during the peak of the long-rains (April) and 52 mm month<sup>-1</sup> during the peak of the short-rains (October), representing 30% and 60% of their long-term means, respectively. The variability over the Juba-Shabelle Basin during October is such that extremes between 1983–2019 have been recorded with a



minimum of just 34 mm month<sup>-1</sup> in 2003 (39% of the long-term mean) and a maximum of 305 mm month<sup>-1</sup> in 1997 (355% of the long-term mean). This variability is driven by various local and remote physical processes, which we now discuss.

## 2.1. Global teleconnections

Rainfall variability over Eastern Africa is influenced by a range of global and regional modes of climate variability (**Fig. 2**), including the El Niño Southern Oscillation (ENSO), the Indian Ocean Dipole (IOD), the Quasi-Biennial Oscillation (QBO) and the Madden-Julian Oscillation (MJO).

The IOD is a key driver of interannual variability across Eastern Africa during the short rains. The positive phase of the IOD is defined by sustained positive SST anomalies in the western Indian Ocean (50°E-70°E, 10°S-10°N) and negative SST anomalies in the eastern Indian Ocean (90°E-110°E, 10°S-0°S), resulting in an SST difference between the two that exceeds +0.4°C. The positive IOD is linked with wetter short rains over Eastern Africa (**Fig. 2**), with precipitation totals that can be 2-3 times the long-term mean<sup>16</sup>, as seen in 1997, 2006, 2012, 2015 and 2019. The negative IOD, defined by a sustained SST difference <-0.4°C, is associated with weaker short rains<sup>17</sup>, resulting in 20-60% of the long-term mean rainfall.

Links between ENSO and Eastern African short rains are also apparent<sup>18</sup>. East Pacific and central Pacific El Niño events typically result in wetter short rains over Eastern Africa, and La Niña conditions result in drier short rains<sup>19</sup> (**Fig. 2**). However, the ENSO impact on Eastern Africa is strongly mediated by the IOD<sup>18</sup>. The typical concurrence of positive IOD with East Pacific El Niño, and negative IOD with East Pacific La Niña, act to amplify precipitation responses, resulting in even larger anomalies across the region. For instance, the coincidence of the 1997 El Niño with a strong positive IOD event led to rainfall anomalies twice the climatological mean values over the short rains season<sup>16</sup>. In contrast, the strong central Pacific El Niño of 2015 coincided with a weaker IOD, producing anomalies ~50% above the climatological mean<sup>18</sup>. However, these relationships are non-linear, as demonstrated by extreme 2019/2020 rainfall that occurred during an anomalously positive phase of the IOD but neutral ENSO conditions<sup>20</sup>.

The IOD and ENSO physically influence Eastern African rainfall by modifying the Indian Ocean Walker Circulation (**Fig. 2**). In the absence of a strong phase of ENSO and IOD during the rainy season, the Indian Ocean Walker Circulation consists of a strong upward branch over the western Pacific warm pool and a much weaker updraft over Eastern Africa. However, when there are unusually warm SSTs over the western Indian Ocean and central Pacific and unusually cool SSTs over Southeast Asia (a positive IOD and El Niño conditions), the Indian Ocean Walker Circulation weakens<sup>21,22</sup>; a strong branch of rising air occurs over the western Indian Ocean and a strong branch of sinking air over the western Pacific. This circulation pattern is associated with elevated rainfall over Eastern Africa. A concurrent positive IOD and El Niño event reinforces these impacts, leading to enhanced rainfall anomalies during short rains over Eastern Africa<sup>18</sup>.

Strong El Niño events can lead to warmer SSTs in the Western Pacific (sometimes referred to as a “Western V Pattern”<sup>23</sup>). Warmer SSTs in the western equatorial Pacific are linked to

drier short rains over Eastern Africa and warmer SSTs in the western North Pacific are associated with dry conditions during the long rains. Warmer SSTs over the western North Pacific strengthen the Walker Circulation that suppresses Eastern African long rains. This SST pattern led to successive dry seasons and droughts across Eastern Africa during 2016-2017 (ref<sup>23</sup>). Variations in the long rains are less sensitive to changes in IOD<sup>24</sup>, since the IOD peaks several months later (during September-November) than the peak in the long rains.

The pan-tropical MJO is a further driver of sub-seasonal rainfall variability over Eastern Africa, influencing both the long and short rains on a monthly basis<sup>25</sup>. The MJO is described in terms of eight phases, corresponding to locations of elevated convection (and rainfall). For example, MJO phases 2-4 are linked with large-scale convection in the Indian Ocean, resulting in westerly wind anomalies and enhanced rainfall<sup>18</sup> (including 22%-78% of extreme rainfall events, depending of MJO phase and amplitude<sup>26</sup>) over the Eastern African highlands<sup>26-28</sup> (**Box 1**). This relationship is weaker in October and April than in November, December, March and May<sup>29</sup>. In contrast, MJO phases 6-8 are associated with suppressed convection across Eastern Africa and the western Indian Ocean, but wet conditions over low-lying coastal regions<sup>26,27</sup>. Greater seasonal rainfall accumulations are observed during a long rains season when the MJO is more active in any phase<sup>30</sup>, with the MJO explaining ~20% of the observed interannual rainfall variations.

Through its relationship with the MJO<sup>31</sup>, the eastward phase of the QBO also influences Eastern African rainfall. Above average long rains are linked to an easterly QBO in the preceding September-November<sup>30</sup>. This six-month lag<sup>32</sup>, is consistent with the time scale associated with the descent of mid-stratospheric wind anomalies to the tropopause<sup>33</sup>. The QBO typically explains <20% of observed interannual rainfall variations, and the strength of this lagged correlation is dependent on which model reanalysis is used<sup>34</sup>, due to model-specific assumptions about convective parameterizations.

### **2.3. Local drivers of variability**

Variations in Indian Ocean SSTs, particularly those in the west that are partially controlled by the IOD<sup>30</sup>, are also linked with variability in both rainy seasons. Warmer SSTs heat the boundary layer leading to anomalous ascent, opposing the climatological subsidence and corresponding drying, thereby enhancing rainfall. Positive SST anomalies in the western Indian Ocean increase the magnitude of short rains over 95% of equatorial Eastern Africa<sup>35</sup>, and explain 9-26% of observed rainfall variations during the long rains<sup>30</sup>. The positive correlation between western Indian Ocean SSTs and rainfall is strongest at the beginning and end of the long rains season<sup>36</sup> when the rainfall is less well established and more susceptible to local and remote forcing. Rainfall during the peak of the long rains (April) is also significantly correlated with southern Atlantic SSTs, whereby cooler SSTs lead to higher rain rates over Kenya driven by zonal winds over central Africa<sup>36</sup>.

The presence of tropical cyclones in the southwest Indian Ocean (when the MJO is in phases 3-4) is associated with low-level westerly anomalies over Eastern Africa, resulting in enhanced rainfall<sup>37</sup>. There is a greater likelihood of westerly flow when the cyclones are located to the east of Madagascar<sup>28</sup>. The cyclone locations and rainfall impacts over Eastern Africa in 2018 and 2019 are consistent with this west/east pattern<sup>37,38</sup>. Cyclones Dumazile and Eliakim in

2018 were located east of Madagascar and were associated with westerly flow and enhanced rainfall, while Cyclone Idai in 2019 was located west of Madagascar and coincided with a drier period<sup>37,38</sup>.

The influence of the Congo airmass, characterized by the 700hPa zonal winds, has also been associated with interannual variability of the long rains<sup>28,36</sup>. Despite climatological easterly winds, westerly winds originating from the Congo sometimes occur during March-May (often linked to phase 3-4 of the MJO<sup>28</sup>), bringing moist air that leads to convergence around Lake Victoria and enhances rainfall<sup>28,36</sup>. Indeed, the cumulative rainfall total of the long rains is further strongly correlated with 700hPa zonal winds across the Congo Basin and Gulf of Guinea. Furthermore, enhanced surface westerlies from the Congo basin, driven by a higher geopotential height gradient over the Congo Basin than the western Indian Ocean, lead to wetter long rains over Tanzania<sup>39</sup>.

### 3 Observed changes in Eastern African rainfall

In addition to interannual variability driven by remote and local drivers, precipitation across Eastern Africa also exhibits decadal-scale trends. Since the early 1980s, a range of satellite-derived rainfall data products have helped to quantify these changes<sup>40,41</sup> (**Fig. 3**). These data products show consistent wetting trends over the Ethiopian highlands (5–12°N, 34–38°E) during March-May (long rains) and the Horn of Africa (2°S–8°N, 35–51°E) during October-December (short rains), with ranges across different datasets of 0.3-1.7 mm season<sup>-1</sup> year<sup>-1</sup> and 1.7-2.7 mm season<sup>-1</sup> year<sup>-1</sup>, respectively (**Fig. 3a, b**). Elsewhere in Eastern Africa, however, rainfall trends based on satellite data are inconsistent in magnitude and sign during both rainy seasons, with the largest discrepancies between data products over the eastern Congo Basin (**Fig. 3a, b**).

In addition to discrepancies between satellite datasets, substantial differences between satellite products and gauge-based records over Eastern Africa add to the uncertainty in estimating long-term spatially resolved seasonal rainfall trends (**Fig. 3c, d**). For example, while satellite records reveal statistically significant trends, gauge-based records, available from the 1950s to 2018, do not display significant trends in precipitation or streamflow<sup>42</sup>. These differences arise from contrasting satellite rainfall estimation methodologies, and spatial and temporal gaps in the rain gauge network<sup>43,44</sup>. However, there is better agreement between areal-weighted rainfall means from different data products in both rainy seasons (**Fig. 3c, d**), particularly after year 2000 when there are fewer gaps in the satellite records<sup>45</sup>, resulting in greater confidence in reported rainfall trends particularly for both the long and short rains.

#### 3.1. Long rains

Over Eastern Africa, consistent negative long rain trends were observed over 1985-2010 (**Fig. 3a, c**). The magnitude of these trends is sensitive to the dataset used, ranging from -0.7 mm season<sup>-1</sup> year<sup>-1</sup> to -1.5 mm season<sup>-1</sup> year<sup>-1</sup>. Particularly marked declines occurred in ~1999 and 2010-2011 (refs<sup>46-49</sup>), the latter event causing devastating droughts in Kenya, Somalia and south-eastern Ethiopia. Trends calculated up until ~2017 also continue to be negative. However, very wet long rains in 2018 and 2020 indicate some recovery (**Figure 3a, c**). Trends computed between 1983-2021 therefore no longer indicate widespread and consistent drying across the Horn of Africa. Instead, less consistency emerges among datasets (**Fig. 3a, c**),

with some indicating a general wetting trend (TAMSAT,  $1.23 \text{ mm season}^{-1} \text{ yr}^{-1}$ ;  $0.47\% \text{ season}^{-1} \text{ yr}^{-1}$ ) and others an overall drying trend (GPCC,  $-0.13 \text{ mm season}^{-1} \text{ yr}^{-1}$ ;  $-0.08\% \text{ season}^{-1} \text{ yr}^{-1}$ ) when considering the period 1983-2019.

Different mechanisms have been proposed to explain this reduction in the long rains up to the 2010s. On the one hand, the decline has been linked to Pacific Ocean SST variability<sup>50–52</sup>. Specifically, Pacific Decadal Variability manifests as a pattern of SST that has a larger latitudinal extent than associated with ENSO, and has been described as a “Western V” pattern that encapsulates warm SST values centred over the western Pacific warm pool with tongues of warm SSTs extending northeastward toward Hawaii and southeastward into the southern central Pacific<sup>23,53</sup>. Warming of Indo-Western Pacific SSTs enhances convection over the western equatorial Pacific leading to an anomalous Walker circulation over the Indian Ocean, strengthening of the upper-level easterlies, increased subsidence over Eastern Africa in the descending branch, and consequently reduced rainfall during the long rains<sup>54,55</sup>. In some instances, the strengthening of the upper-level easterlies has been highlighted as the dominant driver in this process, with minimal connections to Walker Circulation variability<sup>55</sup>. More rapid warming of the West Pacific relative to the East Pacific since 1998, associated with a negative phase of the Pacific Decadal Oscillation<sup>56</sup>, has been linked with a greater susceptibility of the long rains to drought during La Niña events with an increased risk of concurrent short-long rains droughts<sup>23</sup>. Strengthening of the W-E SST gradient across the Pacific since 1998 has led to a stronger Walker circulation and faster Pacific trade winds<sup>57,58</sup> that results in drying over Eastern Africa via Indian Ocean teleconnection, in contrast with coupled climate model simulations<sup>59</sup>.

On the other hand, the shortening of the long rains season<sup>47</sup> (later onset and earlier cessation) from the 1980s to late 2000s has been attributed to the rainfall decline. In this case, faster SST warming in the Arabian Sea compared to further south, enhances the pressure gradient and thus a faster-moving rainband. Declining westerly 700 hPa winds are also linked with the decadal drying trend during the long rains<sup>48</sup>, driven by changes in geopotential height gradient that are associated with increased heating around Arabia and the Sahara<sup>48</sup>. Positive anomalies in westerly winds are associated with enhanced rainfall over Eastern Africa (section 2.3) and conversely declining westerlies are associated with reduced rainfall. Finally, internal variability<sup>47,48</sup>, such as variations in SST that are not linked with radiative forcing, is also thought to be a driver.

### 3.2 Short rains

Compared to the long rains, there is greater consistency in the sign and magnitude of short rain trends (**Fig. 3b, d**). Trends calculated over 1983-2021 are broadly consistent across CHIRPS and TAMSAT, each highlighting an increase in short rain totals of 50-100 mm. We do not report the trend for GPCC because it is not available beyond 2019 but it is consistent with CHIRPS and TAMSAT for the shorter period of 1983-2019. We also do not report the trend for ARC because it includes spurious time-varying jumps<sup>43</sup> that compromise a robust estimate for the trend. Spatially, all datasets exhibit this increasing rainfall trend over large parts of Tanzania, Uganda, Kenya, Somalia and Ethiopia (**Fig. 3b**), ranging  $1.27\text{--}2.58 \text{ mm season}^{-1} \text{ year}^{-1}$  ( $0.92\text{--}1.82\% \text{ season}^{-1} \text{ year}^{-1}$ ).

As with the long rains, regional-mean long-term linear trends in short rains are punctuated with periods of anomalous rainfall. For example, short rain totals during 1997-1998 and 2019-



2020 were 2-3 times higher than climatological values<sup>16</sup>, the former being linked to the El Niño event<sup>49,60</sup> and corresponding connections to the positive IOD, with the largest positive rainfall anomalies of 100-250 mm year<sup>-1</sup> reported in 1997, 2006, 2012, 2015, and 2019 (**Fig. 3d**). This is consistent with earlier analyses<sup>51,52</sup> and with mechanisms that determine year to year variations.

We find that including 2020 and 2021 does not change the spatial pattern of rainfall changes during OND but does increase the magnitude of the wetting trend in the short rains, as it does for the long rains. In general, we find that the regional-mean wetting trend is mostly a result of short-term variability driven by changes in ENSO and the IOD.

### **3.3 Anthropogenic connections**

Large year-to-year variability in the long and short rains discussed in the previous section presents a difficulty in interpreting drivers and isolating the anthropogenic imprint. Paleoclimate reconstructions provide a longer-term view of rainfall changes over Eastern Africa. They show that changes in rainfall in the last century across the globe are not unprecedented in the context of the past two millennia, but the rate at which rainfall is changing is unusual. These data reveal a drying trend over the past two centuries<sup>50</sup> and a recent increase in drought frequency over the Horn of Africa during March-May<sup>61</sup>.

Greenhouse gas-induced warming drives an increase in atmospheric moisture and its convergence which intensify wet seasons while higher temperatures and greater evaporative demand intensify dry seasons, contributing to a greater severity of wet and dry extremes<sup>62</sup>. Cooling from anthropogenic aerosols has partially offset these greenhouse gas changes, and, through an additional altered global distribution of aerosol forcing, have been implicated in a southward shift in the African ITCZ from the 1950s to the 1980s (ref <sup>63</sup>). Recovery from this altered state has been attributed to a combination of greenhouse gas and aerosol forcing<sup>64</sup>. While there is some consensus about the human influence on rainfall over Eastern Africa (via greenhouse gas induced warming and cooling from anthropogenic aerosols<sup>21,64,65</sup>), the anthropogenic influence on the physical processes (specifically the IOD) that control year-to-year rainfall changes is less clear<sup>55,66</sup>. Based on a combined model and data analysis, drought trends over Eastern Africa are most consistent with changes in precipitation rather than increasing temperature<sup>67</sup>.

An increased frequency of the positive phase of the IOD during the second half of the twentieth century has not led to higher seasonal rainfall amounts compared to the first half of the twentieth century<sup>55</sup>. This observation is consistent with understanding of how a warming climate perturbs the thermal structure of the atmosphere and the circulation of the tropical oceans<sup>68,69</sup>, resulting in a long-term weakening of Walker and Hadley circulations and the narrowing of the ITCZ<sup>55,70,71</sup>. Yet, observed strengthening of the Walker circulation since the 1990s, associated with rapid warming of the tropical west Pacific relative to the east Pacific, is not reproduced well by simulations and this has been linked with systematic model biases that may limit the projections of Eastern African rainfall<sup>59</sup>. Therefore, anthropogenic signals of Eastern Africa rainfall are yet to be clearly established in the observational record and future projections assessed in Section 5 should be interpreted in the context of these complex present-day drivers and uncertainties.

## 4 Impacts of observed rainfall variations

Local and remotely driven variability in the short and long rains have substantial and multifarious environmental, humanitarian and economic impacts occurring over various temporal scales. Given the diversity of the impacts of Eastern African rainfall variability, we focus here on three broad groupings of impacts: agriculture, natural ecosystems, water security, and human health. These impacts are not exhaustive but represent a diverse subset of widely researched topics. It is also important to bear in mind that precipitation impacts do not occur in isolation; often such impacts coincide with changes in temperature, complicating explicit attribution to rainfall.

### 4.1. Agricultural impacts

Rainfall variability across Eastern Africa affects agriculture directly and indirectly. Much agriculture in the region is rain-fed. As such, failure of seasonal rains result in agricultural droughts, the frequency of which has increased from once every ten years in the early 1900s to once every three years since 2005 (ref<sup>72</sup>). While small- and large-scale irrigation schemes are helping to mitigate the impacts<sup>73,74</sup>, minimal infrastructure exists to retain, redistribute and store water to cope with this intra-seasonal and interannual variability. The resulting loss of agricultural production has thus been the cause of some of the most well-known humanitarian disasters in the 20<sup>th</sup> and 21<sup>st</sup> centuries, including the 1974 Sahel drought which resulted in an estimated 325,000 deaths, and the 1984 drought across Ethiopia and Sudan that caused 450,000 deaths<sup>75–77</sup>. Since then, Ethiopia has experienced several droughts. One responsible factor is El Niño, which results in contrasting impacts over Ethiopia<sup>78</sup>: lower than normal rainfall over northern Ethiopia that responds similarly to the Sahel region, and higher than normal rainfall over southern Ethiopia that can lead to flooding. Variations in the climate system, e.g., location of the ITCZ, and regional orography (**Box 1**) complicate this relationship.

The 1997/1998 drought over northern Ethiopia, while not as extreme or as widespread as the drought in 1984, illustrates other agricultural impacts. Cereal production<sup>79</sup> declined by 25% during this period, resulting in price increases of 15–45%. This was due to lower crop yields due to drought and indirectly by reduced cultivated land because of malnourished oxen<sup>80</sup>. Reduced crops also caused cattle mortality rates of 26% in some regions due to dehydration/starvation and disease<sup>81</sup>, with cattle typically more affected by drought than camels or small ruminants<sup>82</sup>. Efforts to implement drought early-warning systems<sup>83,84</sup> increase agricultural capacity by distributing drought-resistant seeds, and enhance rapid humanitarian responses from governments and international aid that seek (and have arguably helped) to mitigate deaths associated with food security<sup>85,86</sup>. Humanitarian impacts of the historic drought<sup>87</sup> in 2015 and subsequent droughts<sup>88</sup> in Ethiopia and of the three major droughts over Somalia over the last decade (2011/2012, 2016/2017 and 2021/2022), due to consecutive failed rain seasons, demonstrate the complex and evolving challenges faced by Eastern African countries.

While below normal rainfall threatens agriculture, so does an increase in rainfall intensity. In regions that are moisture limited, benefits from increased rainfall can be expected<sup>89</sup>. However, regions with low permeability soils such as the clay vertisols of the sub-humid regions of Ethiopia that have infiltration capacities of only 2.5 to 6.0 cm/day, the landscape is easily overwhelmed by intensive rainfall<sup>90</sup>. Low permeability of irrigated lands results in waterlogging

and crop damage, and poor drainage systems substantially limit the production potential of the soils<sup>91</sup>. For example, productivity losses of 45% over 60 years have been recorded for some Ethiopian sugar plantations due to waterlogging. Furthermore, the erosion of agricultural topsoil occurs when runoff from sloped terrain exceeds the rate of soil intake<sup>92</sup>, affecting future productivity. An illustration of this is the unusually heavy rainfall over northern Ethiopia during March and April 2016, immediately following extensive drought conditions, which led to widespread flooding, landslides, displacement of people, and damage to crops. Based on recent changes in rainfall over Eastern Africa, there is a growing influence of extreme rainfall seasons that will continue to negatively impact agricultural productivity.

High densities of desert locusts (*Schistocerca gregaria*) also pose a threat to agricultural crops and are strongly linked to rainfall variability. Heavy and extensive rainfall provides moist soil for egg laying, and the subsequent rain-fed flushing of vegetation provides shelter and food for the locusts causing widespread damage. As such, rainfall is a dominant factor governing their population and movement, as evidenced by several documented locust plagues over Eastern Africa<sup>93–96</sup>. The extent of crop damage is related to successfully locating locusts breeding grounds and to proactive interventions that are sometimes compromised by armed conflict<sup>97</sup>. Given rainfall connections to the IOD and ENSO, locust plagues and resulting crop damage typically occur during positive IOD years when rainfall is enhanced<sup>98</sup>, for example, the years 1986/1987, 1992/1993, and 2019/2020. These remote drivers often interact with local drivers. For example, the 2020 locust outbreak—the worst in 25 years for Ethiopia and Somalia and in 70 years for Kenya—has been linked to the rare landfall of two tropical cyclones in the Arabian Peninsula during 2018, exponential growth in breeding through the creation of ephemeral lakes, their southward migration to Eastern Africa, and subsequent establishment of the swarm from IOD-related enhanced vegetation growth. The COVID-19 pandemic along with other factors prevented proactive interventions in this case and resulted in an estimated US\$8.5 billion in crop damage in Yemen and Eastern Africa during 2020, amplifying threats to food security<sup>99</sup>. Indeed, over Ethiopia between December 2019 and March 2020, 114,000, 41,000 and 36,000 hectares of sorghum, maize and wheat were estimated to be damaged<sup>100</sup>, respectively.

SSTs prior to cyclogenesis have got progressively warmer over the north Indian Ocean<sup>101</sup> over the period 1980–2020, facilitating higher heat fluxes from the ocean to the atmosphere that are linked to the frequency and intensity of cyclones. Generally, differential warming of SSTs across the Indian Ocean affects the location of cyclogenesis. Particularly, there has been rapid warming over the Arabian Sea and the Bay of Bengal thereby increasing the chances of the storms reaching land and creating ephemeral lakes that can sustain locust breeding. Indeed, three times the number of cyclones affected the Arabian Peninsula during the 2010s compared with the previous two decades. The frequency of cyclones in the north Indian Ocean is also linked with warmer SSTs over the eastern Indian Ocean associated with the negative IOD pattern<sup>102</sup>.

## **4.2 Ecosystem impacts**

Rainfall variability also has strong bearing on various ecosystem functions, including terrestrial gross primary production (GPP), wildfire activity and wetland emissions of greenhouse gases.

Terrestrial GPP—the total amount of carbon fixed by plants—is closely related to water availability in Eastern Africa’s tropical forest and savannah ecosystems<sup>103</sup>. Tropical African ecosystems are typically more limited by water than sunlight on a regional basis<sup>104,105</sup>. Interannual variations in water availability<sup>103</sup> through rainfall and groundwater result in GPP variations within  $\pm 10\%$  of climatological values. For forest ecosystems, GPP anomalies are highly correlated with changes in groundwater and soil moisture, generally increasing during periods of elevated rainfall, except in regions where annual rainfall exceeds 1800 mm<sup>103</sup>. This decline in productivity with higher rainfall may reflect reduced sunlight due to cloud cover. For savanna ecosystems, rainfall patterns have a stronger influence on inter-annual variability in productivity. Although, productivity in these ecosystems is also controlled by soil moisture and groundwater because shrubs in dry savannas may still have access to below surface water<sup>106</sup> due to their deep rooting systems.

Much less is known about how African ecosystems respond to changes in rainfall than other tropical ecosystems, but models of GPP driven by satellite observations of vegetative properties, rainfall, and groundwater are beginning to improve our understanding. Based on a GPP product<sup>107</sup> inferred from the NASA SMAP satellite instrument, the annual mean GPP for 2003-2017 is  $\sim 3.08 \pm 0.19$  Pg/yr. Drought years of 2005 and 2015 and elevated rainfall in 2010 exemplify the range of GPP responses to rainfall changes that were driven by SST anomalies in the South Atlantic and Indian Oceans. The weak El Niño year of 2005, immediately preceded by years of anomalously low rainfall and depleted groundwater, led to a drop of 5% in GPP over  $-5$ - $10^\circ\text{N}$ ,  $30$ - $50^\circ\text{E}$  ( $-0.15$  Pg/yr). In contrast, in 2015 when there were similarly weak El Niño conditions, anomalously low rainfall, particularly over latitudes  $-10$ - $10^\circ\text{N}$ , was partially offset with groundwater reserves that were replenished in the preceding five years, resulting in a GPP of 3.19 Pg/yr, close to the climatological mean value. During the strong 2010 El Niño, there were widespread increases in GPP across the region ( $+0.15$  Pg/yr, representing +5%) except for parts of the Horn of Africa. Groundwater reservoirs can act as a temporary buffer against drought during years of low rainfall for sufficiently deep rooting systems, but only if they have an opportunity to replenish during anomalously wet years. Regions that suffer from consecutive years of below average rainfall, such as countries in the eastern most part of Horn of Africa, will see drops in GPP and eventually increasing rates of vegetation mortality.

By influencing GPP, rainfall variability can also influence vegetation fire activity and consequently emissions of air pollutants, CO<sub>2</sub> and other GHGs<sup>108–110</sup>. For example, above average rainfall during the growing season increases plant productivity, thereby increasing the fuel load available for burning in subsequent seasons or years<sup>111</sup>. In contrast, above average rainfall during the dry season can suppress fire activity, although fire ignition via lightning is enhanced during moist convection<sup>112</sup>. Both processes have proven to be important in Eastern Africa during initial years of the 21<sup>st</sup> century<sup>113</sup>.

Landscape fires in Eastern Africa are typically focused on South Sudan and parts of western Ethiopia and northern Uganda during January and Tanzania and part of southern Uganda during July. During the 2001-2012 period, changes in rainfall explained about 20% of the negative trends in burned area in South Sudan<sup>114</sup>. Based on ENSO events during 1997-2016, El Niño years lead to a small reduction in burned area anomalies in forest and non-forest ecosystems over northern hemispheric Africa. Generally, ENSO plays a smaller role in burned



area and subsequent emissions than in other tropical biomass burning regions<sup>115</sup>. This is supported by an ensemble analysis of Earth system models (ESMs)<sup>116</sup>.

Tropical wetland emissions of methane, an important greenhouse gas, exhibit marked relationships with precipitation given the dominant control of inundation extent and water table depth<sup>117,118</sup>. Aquatic production of methane is due to anoxic decomposition of organic matter from root systems and decaying plants, influenced by a range biochemical and phenological factors<sup>119–121</sup> and local macrophyte diversity<sup>122,123</sup>.

Satellite data revealed the global significance of Eastern African wetland emissions of methane over South Sudan and western Ethiopia during the long and short rain periods over the last decade<sup>124–127</sup>. Seasonal variations in emissions are controlled by local rainfall, whilst longer-term changes are driven mostly by rainfall collected by upstream catchment areas (for example, Lake Victoria, Lake Albert). Water released from these catchments is transported downstream via the White Nile leading to demonstrable increases in wetland extent and associated vegetation flushing, particularly over the Sudd<sup>128,129</sup>. Wetland emissions from the Sudd in South Sudan during 2010–2016 represented about a third of the global atmospheric growth of methane. A strong positive phase of the IOD during 2018–2019 led to anomalously large rainfall totals over Uganda and Kenya during March–May 2018 and October–December 2019, equivalent to a once in 30-year event<sup>130</sup>. The additional methane emissions due to the anomalous short rains in 2019, focused on South Sudan and Ethiopia, represented a quarter of the global atmospheric methane growth rate for that year<sup>130</sup>. The anomalous global atmospheric methane growth rates in 2020 (ref<sup>131,132</sup>) and 2021 (ref<sup>132</sup>) have also been partly attributed to anomalous Eastern African wetland emissions.

Wetlands can also be hotspots of ammonia (NH<sub>3</sub>) gas emissions<sup>133,134</sup>. Ammonia is a precursor to the formation of secondary inorganic aerosols, which are the main contributor to particulate matter globally and represents a hazard to human health<sup>135,136</sup>, and its deposition to downwind ecosystems can lead to eutrophication, soil acidification, reduced productivity, biodiversity decline, and indirect GHG emissions<sup>137–140</sup>. Ammonia is volatilized from ammonium in soils via an abiotic reaction, which is influenced by pH, temperature, and, of importance here, soil moisture content linked to changes in rainfall. When soils with high moisture content start to dry out, NH<sub>3</sub>-nitrogen tends to become more concentrated at the same time as there are reduced limits on gas diffusion through soils, which, along with other factors, leads to enhanced NH<sub>3</sub> emissions<sup>141–143</sup>.

These processes have been shown to produce a large seasonal increase in NH<sub>3</sub> concentrations ( $8 \times 10^{15}$  to  $13 \times 10^{15}$  molecules cm<sup>-2</sup>) over salt flats in Tanzania as the waters of Lake Natron, a soda lake with relatively alkaline pH, recede during the dry season<sup>144</sup>. A similar seasonal behaviour has been observed over the Sudd wetlands in South Sudan<sup>145</sup>. Roughly half of the Sudd wetlands are permanently flooded, with part of the remaining wetland area drying each year<sup>146</sup>. The extent of drying can vary substantially from year to year. For example, NH<sub>3</sub> concentrations over the region reached nearly  $30 \times 10^{15}$  molecules cm<sup>-2</sup> in 2010 when seasonal drying of the Sudd was most extensive, compared with  $11 \times 10^{15}$  molecules cm<sup>-2</sup> in 2014 when drying was least extensive<sup>145</sup>.

#### **4.3. Water security**

Rainfall variability has direct consequences for human wellbeing and health, including generation of clean energy from hydropower, transboundary water management, urban drainage, and vector-borne and water-borne diseases. A preliminary assessment by the UN in 2022 of water security across Africa<sup>147</sup>, based on a range of ten criteria including access to drinking water, sanitation, and water infrastructure, highlighted that Eastern Africa includes some of the lowest scoring countries.

To meet growing energy demands in Eastern Africa, hydropower development is often seen as a viable solution and one that does not involve the combustion of fossil fuels. Ethiopia and Sudan seek to meet domestic energy needs and aspire to market energy across the East Africa Power Pool (EAPP). The current capacity of hydropower contributes about 50% of electrical generation in EAPP countries, with a planned doubling of capacity over Eastern Africa by 2030 that will mostly be in the Nile Basin. However, a strong dependency on hydropower places the entire economic system at the mercy of variable hydrologic conditions<sup>148</sup> in an increasingly uncertain climatic future<sup>149,150</sup>. Linking energy networks across hydrologic zones and organising infrastructure investment to be ‘climate-proof’ is one potential solution, without which countries that rely heavily on hydropower will likely suffer from fluctuating electricity prices<sup>148</sup>. The EAPP may help to coordinate the trade and interconnection of cross-border energy networks, but there remain significant political challenges as energy needs grow with projected future increases in urbanisation, expanding irrigation plans, and variable release from upstream hydropower plants<sup>148,151</sup>.

While Zambia is not part of Eastern Africa it does serve as an example of the multiplicative consequences of rainfall variations on hydropower, and they are part of the southern African counterpart of the EAPP. Extremely dry conditions during 2015 and 2016 linked with the strong El Niño led to reduced inflow into Lake Kariba that feeds into the Kariba Dam that provides 1,830 megawatts of hydroelectric power to Zambia and Zimbabwe. Lake levels in January 2016 dropped to 12% of capacity, just above the minimum necessary to generate electricity<sup>152</sup>. This led to major energy deficit in Zambia that was managed by buying energy from neighbouring countries and daily power outages, particularly affecting Lusaka Province and the Copper Belt. This subsequently led to damages associated with a suspension of heating and refrigeration and, combined with a fall in global copper price, led to an estimated 19% drop in GDP<sup>153</sup>. Conversely, anomalous flooding of the Zambezi basin due to torrential rainfall can overwhelm the Kariba Dam resulting in a necessary release of water. This occurred in March 2010 due to El Niño conditions, affecting the discharge rates of downstream dams, leading to major floods that impacted hundreds of thousands of people.

More generally, variability in precipitation presents an important issue for regional water security in Eastern African countries that include transboundary rivers<sup>154</sup>. There are substantial challenges associated with managing critical multi-purpose infrastructures that support dams for hydropower but also for agricultural expansion and flood control, especially considering variations in rainfall and the associated river flows. Safely handling severe flooding and drought events requires close communication between managers of different dams, some of which will be across political borders, to avoid harm to co-riparian nations<sup>155</sup> and to avert international conflict<sup>156</sup>.

Fortunately, violent conflict between nations over shared water resources is almost non-existent anywhere on the globe<sup>157</sup>. Over Eastern Africa, minor conflicts have been mainly led by herders and farmers in neighbouring countries fighting over pasture and water for livestock. Construction of the Grand Ethiopian Renaissance Dam (GERD) on the Blue Nile River has the potential to be the biggest risk of conflict between neighbouring Eastern African countries<sup>155</sup>. The dam is part of Ethiopia's economic growth plan to become Africa's largest hydropower exporter. However, there is concern that GERD will reduce downstream water for irrigation and drinking, and to a lesser extent reduce hydropower capacity. Years of heavy rainfall over Ethiopia, such as 2020, can help fill the GERD and result in release of sufficient water to Sudan and Egypt<sup>158</sup>. Proponents of GERD argue that in years with lower rainfall, the dam's water storage can be used to alleviate drought in downstream countries. But this relies on the dam releasing the water. Diplomatic negotiations are ongoing, but the situation serves as an example of the complexities associated with transboundary water.

Economic development of Eastern African countries is tied to increasing urbanization, resulting in rapid expansion of cities to accommodate growing populations<sup>159</sup>. This includes expansion of infrastructure to support access to electricity and clean water, removal of wastewater and sewage treatment, development of road networks, and improved internet and cellular connectivity. Periods of intense rainfall can quickly overwhelm inadequate infrastructure<sup>160</sup>, resulting in overflowing drainage systems, flooded houses and suspension of sewage treatment that often leads to a range of health emergencies<sup>161</sup>. Flooding can also damage roads and railways built with limited budgets and inadequate engineering, disrupting the transportation of workers and food supplies from rural to urban areas and consequently affecting economic activity<sup>162</sup>.

Heavy rainfall over Sudan in 2020 led to extensive flooding that damaged or destroyed 112,000 homes, causing a three-month state of emergency to be declared<sup>163</sup>. Heavy rains and flash flooding over Sudan in 2021 affected 88,000 people in 13 out of the 18 states. Damage and destruction of houses and clean water sources were widespread. Flash flooding also affected the sewage systems of internally displaced persons camps in South Darfur, closed schools, power plant substations, and rendered roads impassable. The frequency and magnitude of heavy rainfall across Sudan will continue to prove a challenge for urban areas that do not have adequate infrastructure and will ultimately compromise the economic development of the region.

#### **4.4. Human Health Impacts**

Rainfall is also a key component for the propagation of several vector-borne and water-borne diseases relevant to Eastern Africa. The influence of temperature on the malaria parasite, for example, is well understood<sup>164–166</sup> compared to the impact of intense rainfall and associated flooding on the mosquito life cycle and subsequent virus transmissions. Mosquitoes and other arthropods that carry malaria and arboviruses such as dengue, often include an aquatic stage to support the development of their eggs and larvae. A number of studies have focused on extreme rainfall events during the El Niño phase of ENSO during 1997/1998 and 2015/2016<sup>167–170</sup>. Other studies have linked the IOD to an increase in the risk of malaria in the Eastern African highlands<sup>171,172</sup>. There are similar challenges associated with water-borne diseases such as cholera and typhoid that are prevalent across Eastern Africa, and become

of more concern during specific shifts in rainfall and variations in temperature<sup>162,173,174</sup>. Combatting these viruses is exacerbated by non-climate factors, including international travel, pockets of increased population density associated with urbanisation, and land-use change that can move peri-urban regions closer to mosquito and arthropod breeding grounds.

Extreme rainfall associated with the strong El Niño during 1997/1998 followed an extended drought period and led to an outbreak of malaria in a non-immune population of north-eastern Kenya, the extent of which had not been seen since 1952. Records of hospital admissions reported a three-month lag after heavy rainfall in November 1997 (ref<sup>167</sup>). Hospital data from one community reported a ten-fold increase in expected daily rates of crude and under-five mortality<sup>167</sup>, which rapidly reduced by the end of April 1998 when rainfall subsided. A similar story was reported for a district in western Uganda<sup>168</sup>. For communities of the Tanzanian highlands, however, researchers found a marked reduction in malaria cases in 1997/1998 compared to previous years. This reduction was attributed to flooding that can flush mosquito larvae from breeding sites thereby decreasing the disease spread<sup>175</sup>. Two out of the three communities that reported an increase in malaria after the heavy rains were located next to a body of standing water that is an ideal breeding ground for mosquitoes<sup>175</sup>. More generally, periods of heavy rainfall, irrespective of whether they are associated with El Niño or the IOD, result in human health challenges for local communities that are overwhelmed by floods that lead to pools of standing water<sup>169,170</sup>.

We have described a few of the many impacts associated with rainfall extremes over Eastern Africa. Trends and variations in rainfall are linked with, and therefore difficult to separate from, changes in temperature. Concurrent changes in temperature<sup>176–178</sup> can reinforce or weaken<sup>179</sup> impacts due to rainfall.

## 5 Future changes

Given the multifarious impacts of rainfall changes over Eastern Africa, there is a need to consider how rainfall and its drivers might change in the future. This knowledge provides actionable information with which to develop effective mitigation strategies.

### *Rainfall*

Projected future changes in Eastern African climate have been studied using global and regional climate models<sup>20,50,180–186</sup> (GCMs and RCMs, respectively), each with considerable spread amongst ensemble members and models, casting doubt on the reliability of projections<sup>59</sup>. Unfortunately, there are also limited relationships between the abilities of individual models to describe past and future Eastern African climate and the model spread<sup>187</sup>. Hence, constraining future projections simply by observation of current day ESM performance is not possible.

These model limitations are particularly evident for the long rains when GCMs and RCMs show substantial inter- and intra-model differences, resulting in a diversity of projected responses and thus uncertainty. Indeed, GCMs report no significant change<sup>184</sup>, a decrease<sup>188</sup> and a small increase in the long rains under anthropogenic warming, consistent with the range of responses for CMIP5 models<sup>181,189</sup>. CMIP6 simulations also exhibit variability, with the



multi-model ensemble providing hints of a small increase in the long rains for Eastern Africa (the sum of IPCC southeast and northeast Africa regions) (**Fig. 4a**). Under Shared Socioeconomic Pathway 2-4.5 (SSP2-4.5), for example, the multi-model median projects statistically significant  $0.02 \text{ mm day}^{-1} \text{ decade}^{-1}$  increases (2015-2100), although changes only really emerge after  $\sim 2080$ . These increases are also sensitive to the emission scenario used, as demonstrated by a larger positive trend ( $0.06 \text{ mm day}^{-1} \text{ decade}^{-1}$ , 2015-2100) under SSP5-8.5 (**Fig. 4b**), which also tend to emerge earlier ( $\sim 2040$ ). In contrast, CORDEX<sup>190</sup> regional models support no such increase in the long rains, instead exhibiting a statistically significant slight negative trend for Representative Concentration Pathway 4.5 (RCP4.5;  $-0.01 \text{ mm day}^{-1} \text{ decade}^{-1}$ , 2006-2100; **Fig. 4c**), and a statistically insignificant slight positive trend for RCP8.5 (**Fig. 4d**). Based on these calculations, there is no clear indication regarding the sign and magnitude of future long rain changes over Eastern Africa, nor their potential drivers. These minimal changes in long rains have been attributed to the continental thermal low, centred near the equator and present during the long rains, being insensitive to changes in subtropical atmospheric hydrodynamics driven by rising atmospheric GHG during the 21<sup>st</sup> century<sup>15</sup>.

These models generally exhibit better inter- and intra- model agreement for the short rains<sup>181</sup>, albeit still with substantial spread, providing some confidence in the projected future climate states. Indeed, the short rains are projected to increase with anthropogenic warming<sup>20,184,188</sup>. Under SSP2-4.5, the CMIP6 ensemble projects a statistically significant  $0.04 \text{ mm day}^{-1} \text{ decade}^{-1}$  (2015-2100) increase in the short rains, the increase emerging in the early 2040s (**Fig. 4a**). These changes are more pronounced under SSP5-8.5 for the same period, wherein trends of  $0.11 \text{ mm day}^{-1} \text{ decade}^{-1}$  are projected, emerging earlier<sup>20</sup> in the 2030s (**Fig. 4b**). CORDEX simulations exhibit a similar pattern: a small but statistically significant increase for RCP4.5 ( $0.03 \text{ mm day}^{-1} \text{ decade}^{-1}$ , 2006-2100; **Fig. 4c**), and a stronger response that emerges in the late 2040s for RCP8.5 for the same period ( $0.05 \text{ mm day}^{-1} \text{ decade}^{-1}$ ; **Fig. 4d**). A convection-permitting regional model also supports these findings, additionally reporting a large increase in extreme rainfall rates during the short rains<sup>191</sup>. The magnitude and large spatial extent of this increase in extreme rainfall were underestimated by the corresponding regional models using parametrised convection (including CMIP5, CMIP6 and CORDEX simulations) so they may be underpredicting the full extent of future increases in rainfall intensity across Eastern Africa<sup>191</sup>.

This increase in the short rains arises from increased moisture convergence over Eastern Africa<sup>15</sup>. This enhanced moisture convergence emerges from increased atmospheric moisture<sup>184</sup> due to a warming climate and from anomalous circulation patterns associated with a strengthening in the continental low over southern Africa and the subtropical high over the South Indian Ocean, and a weakening of the eastern Sahara subtropical high. A weakening of the Walker circulation in response to warming SSTs over the western Indian Ocean also favours an upward trend in the short rains<sup>50,188</sup>. Nevertheless, limitations in model representations of key processes and climatologies, for example, overestimates in the short rains and underestimates in the long rains<sup>192</sup>, an unrealistic dominance of the Walker circulation<sup>193</sup>, and failure to reproduce the observed SST gradient across the equatorial Pacific<sup>59</sup>—all cast doubts on rainfall projections and understanding of their corresponding drivers. With these caveats in mind, conclusions are limited to saying that the rainfall during the short rains is increasing at a faster rate than the long rains (**Fig. 4**).

## ENSO and IOD

ENSO and the IOD have had a dominant influence on rainfall variations across Eastern Africa. It is therefore instructive to understand their future projections in the hope of informing rainfall projections. As with rainfall itself, there is often a lack of consensus regarding how these modes of variability will change under anthropogenic warming. For ENSO<sup>194</sup>, no significant change in intensity and frequency has been reported in some instances<sup>195–197</sup>, while an increased occurrence of extreme El Niño and La Niña events is reported by others<sup>198–200</sup>. Similarly, no significant change in the overall frequency and amplitude of the IOD is projected by coupled models<sup>201,202</sup>, although the frequency of extreme positive IOD events is thought to increase<sup>198,203</sup>. Assuming present-day relationships between Eastern African rainfall and ENSO and IOD remain the same in the future, the short rains would then become wetter with an increasing chance of torrential rains and associated higher risk of flooding, but also the potential for groundwater recharge<sup>4</sup>.

However, even if the frequency and intensity of ENSO and IOD do not change in a warming climate, there is some consensus about how these climatic modes of variability will remotely influence the future climate system. For instance, rainfall extremes associated with ENSO and IOD can be expected to be more severe in a warming world owing to an intensified hydrologic cycle<sup>204</sup>. Moreover, faster warming is expected in the western Indian Ocean compared to surrounding bodies of water<sup>198,201,205</sup>. Because of these shifts, the tropical oceans will tend towards an El Niño-like and positive IOD-like state, associated with weakening of the Walker circulation, shifts in the ITCZ<sup>206</sup> and an increase in atmospheric moist static energy. Consequently, as a result of changing background SSTs and circulation shifts during the short rains later this century, ENSO and IOD are expected to have a stronger coupling with rainfall over the Horn of Africa but a weaker coupling with rainfall over the southern part of Eastern Africa<sup>188</sup>. The long rains, which are historically insensitive to remote SST forcing, would then become substantially more responsive to ENSO in future projections<sup>188</sup>. Model projections also suggest an enhanced La Niña-related rainfall anomaly over Eastern Africa during July–September compared to the present period<sup>188</sup>.

Uncertainty about future changes in ENSO and IOD, combined with potential changes in the strength of teleconnections results in considerable uncertainty around changes in future rainfall over Eastern Africa driven by ENSO and the IOD. If the frequency of extreme positive IOD events increases<sup>198,203</sup>, and the strength of the teleconnection increases over the eastern part of Eastern Africa<sup>188</sup>, this may result in wetter conditions over the eastern half of the region during the short rains. Changes in the frequency of El Niño and La Niña events, coupled with increasing sensitivity to ENSO during the long rains and summer rainfall seasons may lead to increasing variability in these seasons in the future. Additionally, increases in the frequency of extreme El Niño and La Niña events, and increasing teleconnection strength, may increase the frequency of extreme rainfall seasons throughout the year.

### *Impacts*

As in the present climate, any future changes in seasonal rainfall across Eastern Africa will result in a wide range of economic and humanitarian impacts.

Changes in agricultural yields due to changing rainfall patterns are crop specific. Based on current understanding, future crop yields are more sensitive to uncertainties in temperature

than rainfall<sup>177</sup> due to crops generally having an optimal growing temperature range, outside of which the yield falls off rapidly<sup>178,207</sup>. Optimal yields also rely on adequate soil moisture that helps to regulate available water in the plant root zone<sup>208</sup>. Changes in the timing, duration, and magnitude of the long and short rains (Figure 4) will also need to be considered by farmers when they decide which crops and seed-types are grown throughout the year<sup>209</sup>. Increased frequency of extreme rainfall events will result in flooding that leads to damaged crops<sup>16</sup> and agricultural infrastructure that raises concerns about food security. Availability of water and food will also influence livestock production<sup>210</sup>.

Anthropogenic warming will also induce changes to large-scale biogeochemical cycles across Eastern Africa, with the possibility to feedback on atmospheric GHG concentrations<sup>127</sup>. Indeed, the influence of rainfall variability on wetland methane emissions is expected to continue in the future. For instance, CMIP5 simulations (Supplementary Information) predict methane emissions will increase by ~4Tg yr<sup>-1</sup> under RCP4.5 and ~11 Tg yr<sup>-1</sup> for RCP8.5 from 2000 to 2100 (**Fig. 5a, b**). These projected increases can be linked to increases in surface temperature, inundation (via rainfall) and net primary production (also indirectly affected by rainfall), each with similar importance (**Fig. 5c**). Moreover, future rainfall variability, namely the projected increase in short rains, is expected to reduce the spatial extent of fires<sup>211</sup> and enhance above-ground biomass (and associated vegetation greening<sup>212</sup> and increase in NPP<sup>213</sup>) with an accompanying transition to forest biomes over Eastern Africa<sup>214–216</sup>. These changes will each have subsequent effects on ecosystem functioning, carbon cycling and broader biogeochemical storylines in the Earth System.

There is a threshold of relative humidity (and temperature) that limits the transmission of malaria and arboviruses via their influence on the associated vectors (for example, mosquitoes) and pathogens<sup>173,217,218</sup>. Increases in relative humidity associated with more extreme wet seasons in the future can shorten the incubation and blood-feeding stages<sup>218</sup> of the mosquito life cycle, but the net impact of these changes is unclear. Increased future levels of rainfall and its variability may also lead to more frequent and persistent flooding that will help establish more breeding sites for insects, although some vectors breed indoors and will be unaffected directly by flooding. The relationship between flooding and water-borne diseases such as cholera and typhoid differs by region<sup>173,217</sup>. However, one of the biggest risks for future transmission of malaria and arboviruses in Eastern Africa is drug and insecticide resistance combined with warmer temperatures and lower relative humidity associated with climate change in the highland regions, where there is little immunity and insufficient health infrastructure<sup>165,166,219,220</sup>.

## 6 Summary & future perspectives

Eastern Africa suffers extreme seasonal and year-to-year variations in rainfall, driving substantial environmental, social, and economic impacts. For instance, extreme changes in hydroclimatic conditions during 2021, exacerbated by water management challenges, have led to some of the worst flooding in South Sudan for the past sixty years, impacting food and energy security, access to potable water, and the spread of waterborne disease and arboviruses. Other parts of Eastern Africa, particularly countries in the Horn of Africa, are experiencing prolonged and extensive drought due to consecutive La Niña events from 2020–2022, exacerbated by GHG warming over the western Pacific. These droughts have resulted

in the collapse of agricultural crops and livestock that support subsistence farming across the region.

While uncertain, there is some consensus that short rains totals (OND) will exceed those of the long rains (MAM) in a warming climate, the timing of which is dependent on the scenario but could occur as early as 2030. Regional climate models generally show a stronger rainfall response to a warming climate, with models that resolve convection reporting even higher extreme rainfall rates. This suggests that the vast majority of climate models, which still use parametrised convection, are potentially underestimating future increases in rainfall and therefore the subsequent impacts across Eastern Africa.

To minimize the risks associated with extreme variations in rainfall over Eastern Africa, several priority areas of future research are required, all demanding the development of proactive policies.

#### Improve meteorological observing networks and forecast systems

Improved early detection and weather forecast systems that focus on Eastern Africa will engender better preparedness for extremes associated with seasonal changes in rainfall and will inform decadal planning strategies. Development and evaluation of convective-permitting regional climate models<sup>191</sup> would provide further confidence in their ability to describe extreme rainfall events that have disproportionately important impacts. Growing model skill in sub-seasonal rainfall forecasts<sup>221–227</sup> relies on improving model physics of the atmosphere and ocean and on more and higher-quality data, particularly from satellites that include instruments that observe atmosphere and ocean properties. Improved model simulations of the long rains over Eastern Africa hinge on improving knowledge of the atmospheric state, particularly humidity, over the Northwest Indian Ocean<sup>228</sup>, which could be tested with a dedicated measurement campaign. Ocean interior measurements currently collected by arrays of buoys across the tropics, particularly the Indian Ocean and western Pacific, could be expanded to help reduce knowledge gaps<sup>229</sup>. To improve forecast skill of high-impact weather events over Eastern Africa, targeted<sup>230</sup> ground-based, airborne and shipborne observations could be deployed to supplement existing operational data streams. Equally important are the assimilation methods that optimise the use of these observations for improving model simulations<sup>231</sup>. Rescuing and sharing historical data over Africa would also improve climate predictions<sup>232</sup>.

Translating forecast analyses into actionable information is a key part of any system<sup>233,234</sup>. The Famine Early Warning Systems Network<sup>83</sup> is a good example of such a system. Delivering useful information to countries requires detailed knowledge about national agricultural and economic policies, evolving national political environments and the capability to communicate with local farming communities and governments. Establishing long-term funding that supports civilian data collecting, transcending lifecycles of individual governments, will help to provide effective information about how to mitigate the worst climate impacts.

#### Improve environmental observing systems

Climate and weather forecast data can also help with disease forecasting<sup>164</sup> but this has not been fully realised. Satellite observations of surface temperature, humidity and land use change can be used to predict shifts in disease burden<sup>235</sup> and hotspots for emerging zoonotic



diseases and how they will spread<sup>236–238</sup>, and together with epidemiological data could form the basis of early detection systems over Eastern Africa<sup>164</sup>.

Understanding quantitative changes in hydrology and the carbon cycle across Eastern Africa is currently limited to very few surface sites and broad inferences from satellite observations<sup>124,239</sup>. Given the importance of water flows across the regions and subsequent impacts on water and food security and the carbon cycle there is a clear need for a more coordinated and sustainable measurement network to monitor variations<sup>240</sup>. More collaboration between African and international hydrologists, ecologists, and carbon cycle scientists will help facilitate this kind of activity.

#### Advance Earth System Models

Exploiting advances in observing systems and better understanding the carbon-water nexus must translate into commensurate improvements<sup>233</sup> in physically based simulations of Eastern African climate, and how it relates to the broader climate system. A key recommendation is to develop a more robust understanding of the relationship between future levels of atmospheric GHG and changes in the frequency and variability of the IOD<sup>69,198,201,203,241,242</sup>, and how future changes in ENSO and the IOD will influence rainfall over Eastern Africa<sup>188</sup> and in turn how that influences vegetation cover and subsequently the emission of methane<sup>127</sup>. This point ties together the previous recommendations, and only by bringing together communities involved in measurements and model development can meaningful progress be made with identifying and prioritizing work on reducing uncertainty.

#### Improve freshwater security

Eastern Africa encompasses regions that are being flooded and regions that are subject to drought, both driven by large inter- and intra-seasonal changes in rainfall. In both extremes, there is an urgent need to improve national water storage infrastructure, flood protection and sanitation systems to improve the safety and security of freshwater resources to help increase agricultural output and a growing population<sup>243</sup>. This is a systemic challenge that requires co-development of water usage strategies between stakeholders and development agencies, informed by scenarios that account for changes in rainfall, land use, and the growing demands from an increase in population. Recommendations include investment in water-saving technologies and efficient management options such as the adoption of sprinkler and drip irrigation systems to replace commonly-used flood irrigation, and to invest in recycling wastewater when surface or groundwater reserves are insufficient<sup>243</sup>. Such an approach should also consider upstream and downstream water demands and losses, including the reduction of evaporative losses, particularly from catchment lakes and reservoirs in arid regions<sup>244</sup> and the potential challenges and implications of adopting different approaches<sup>245</sup>.

#### Ensure food security

Ensuring future food security is related to the security of freshwater, with the agriculture sector generally having the lowest water use efficiency of all the water-using sectors<sup>246</sup>. How this sector will cope with changes in rainfall variability will depend on the nature of those changes. An upward trend in rainfall in some countries for different seasons, with an accompanying warming trend, may benefit some food crops that have a higher optimal growing temperature. However, if increased rainfall results from a higher frequency of extreme rainfall events that follow periods of drought, then flooding will become more of a challenge. Investment in better drainage systems is one solution, but in the longer term an increase in flooded areas that can

be managed may provide an opportunity to increase the use of floodplain agriculture, spate irrigation<sup>247</sup> or inundation canals. A shift in rainfall and surface water catchment areas may result in a redistribution of crops being grown across Eastern Africa. Countries that will suffer from more extensive droughts have other challenges to face. In this case, the agricultural sector should invest in strategic rainwater and surface water storage options that provide reliable flows but incur minimal additional losses, more efficient water management systems, as described above, and distributing drought-tolerant seeds<sup>248</sup> to maximize agricultural crop yields during drought years. Widespread adoption of conservation tillage methods would reduce water and soil loss, mainly by decreasing the intensity of the tillage and retention of post-harvest plant residue<sup>249</sup>. Development of agricultural strategies to help farmers maximize food production during good years would help mitigate impacts during drought years. Institutes affiliated with the Consultative Group on International Agricultural Research continue to play a key role in addressing those sustainable agricultural challenges.

All these recommendations require unprecedented levels of coordination and substantial financial investment to link local to national scales, and in many cases will require trans-boundary cooperation that will also involve extensive international diplomacy. Some activities are underway, but some countries may require international financial aid to establish larger activities that will eventually become self-sustaining. Without properly addressing the bigger challenges now it becomes progressively more difficult for Eastern African countries to cope with future variations in rainfall without incurring substantial humanitarian and economic costs<sup>250</sup> that will dwarf the multi-trillion dollar cost of the Covid-19 pandemic.

## Acknowledgements

P.I.P., L.F., M.L. and R.P.A. acknowledge support from the UK National Centre for Earth Observation (NCEO) funded by the National Environment Research Council (NE/R016518/1). C.W. acknowledges funding of the Grantham Research Fellowship from the Grantham Foundation. K.W. acknowledges Oxford Martin Programme on Transboundary Resource Management. M.G. acknowledges the Coproduction of Climate Services for East Africa project. B.D. and K.H. acknowledge support of the NCEO LTS-S and International Programme (NE/X006328/1).

## Author contributions

P.I.P. originated the review and coordinated the writing. P.I.P., C.M.W., B.D., R.I.M., K.G.W., N.G., J.E.H., N.M. and S.S.F. led the writing of individual subsections, with contributions from R.P.A., C.M.W., B.D., R.I.M., N.G. and S.S.F. provided the figures. All authors helped to revise and refine earlier drafts.

## Competing interests

The authors declare no competing interests.

## References

1. Gamoyo, M., Reason, C. & Obura, D. Rainfall variability over the East African coast. *Theor. Appl. Climatol.* **120**, (2015).
2. Conway, D., Dalin, C., Landman, W. A. & Osborn, T. J. Hydropower plans in eastern and southern Africa increase risk of concurrent climate-related electricity supply disruption. *Nat. Energy* **2**, 946–953 (2017).

3. Ferrer, N. *et al.* Groundwater hydrodynamics of an Eastern Africa coastal aquifer, including La Niña 2016–17 drought. *Sci. Total Environ.* **661**, (2019).
4. Adloff, M. *et al.* Sustained Water Storage in Horn of Africa Drylands Dominated by Seasonal Rainfall Extremes. *Geophys. Res. Lett.* **49**, e2022GL099299 (2022).
5. Taylor, R. G. *et al.* Evidence of the dependence of groundwater resources on extreme rainfall in East Africa. *Nat. Clim. Chang.* **3**, (2013).
6. Food Security and Nutrition Analysis Unit and Famine Early Warning System Network. Somalia FSNAU Food Security & Nutrition Quarterly Brief - Focus on Post Gu 2017 Season Early Warning. (2022).
7. World Bank Group. *Somalia drought impact and needs assessment : synthesis report.* (2018).
8. Food Security and Nutrition Analysis Unit. Somalia faces Risk of Famine (IPC Phase 5) as multi-season drought and soaring food prices lead to worsening acute food insecurity and malnutrition. <https://fsnau.org/node/1947> (2022).
9. UN Office for the Coordination of Humanitarian Affairs. *Horn of Africa Drought: Regional Humanitarian Overview & Call to Action.* (2022).
10. UN OCHA. *Humanitarian Needs Overview South Sudan. Humanitarian Programme Cycle 2021* (2021).
11. Thomas, E. A. *et al.* Quantifying increased groundwater demand from prolonged drought in the East African Rift Valley. *Sci. Total Environ.* **666**, (2019).
12. Elagib, N. A. *et al.* Debilitating floods in the Sahel are becoming frequent. *J. Hydrol.* **599**, 126362 (2021).
13. Adhikari, U., Nejadhashemi, A. P. & Woznicki, S. A. Climate change and eastern Africa: a review of impact on major crops. *Food Energy Secur.* **4**, 110–132 (2015).
14. Megersa, B. *et al.* Livestock Diversification: An Adaptive Strategy to Climate and Rangeland Ecosystem Changes in Southern Ethiopia. *Hum. Ecol.* **42**, (2014).
15. Cook, K. H., Fitzpatrick, R. G. J., Liu, W. & Vizy, E. K. Seasonal asymmetry of equatorial East African rainfall projections: understanding differences between the response of the long rains and the short rains to increased greenhouse gases. *Clim. Dyn.* **55**, (2020).
16. Wainwright, C. M., Finney, D. L., Kilavi, M., Black, E. & Marsham, J. H. Extreme Rainfall in East Africa October 2019 - January 2020 and context under Future Climate Change. *Weather (under Rev.* (2020).
17. Black, E., Slingo, J. & Sperber, K. R. An observational study of the relationship between excessively strong short rains in coastal East Africa and Indian ocean SST. *Mon. Weather Rev.* **131**, (2003).
18. MacLeod, D., Graham, R., O'Reilly, C., Otieno, G. & Todd, M. Causal pathways linking different flavours of ENSO with the Greater Horn of Africa short rains. *Atmos. Sci. Lett.* **22**, (2021).
19. Indeje, M., Semazzi, F. H. M. & Ogallo, L. J. ENSO signals in East African rainfall seasons. *Int. J. Climatol.* **20**, (2000).
20. Wainwright, C. M., Marsham, J. H., Rowell, D. P., Finney, D. L. & Black, E. Future changes in seasonality in east africa from regional simulations with explicit and parameterized convection. *J. Clim.* **34**, (2021).
21. Nicholson, S. E. Long-term variability of the East African 'short rains' and its links to large-scale factors. *Int. J. Climatol.* **35**, (2015).
22. Jiang, Y., Zhou, L., Roundy, P. E., Hua, W. & Raghavendra, A. Increasing Influence of Indian Ocean Dipole on Precipitation Over Central Equatorial Africa. *Geophys. Res. Lett.* **48**, (2021).
23. Funk, C. *et al.* Examining the role of unusually warm Indo-Pacific sea-surface temperatures in recent African droughts. *Q. J. R. Meteorol. Soc.* **144**, (2018).
24. Shaaban, A. A. & Roundy, P. E. OLR perspective on the Indian Ocean Dipole with application to East African precipitation. *Q. J. R. Meteorol. Soc.* **143**, (2017).
25. Zaitchik, B. F. Madden-Julian Oscillation impacts on tropical African precipitation. *Atmospheric Research* vol. 184 (2017).

26. Pohl, B. & Camberlin, P. Influence of the Madden-Julian Oscillation on East African rainfall. II. March-May season extremes and interannual variability. *Q. J. R. Meteorol. Soc.* **132**, (2006).
27. Pohl, B. & Camberlin, P. Influence of the Madden-Julian Oscillation on East African rainfall. I: Intraseasonal variability and regional dependency. *Q. J. R. Meteorol. Soc.* **132**, (2006).
28. Finney, D. L. *et al.* The effect of westerlies on East African rainfall and the associated role of tropical cyclones and the Madden–Julian Oscillation. *Q. J. R. Meteorol. Soc.* **146**, (2020).
29. Berhane, F. & Zaitchik, B. Modulation of daily precipitation over East Africa by the Madden-Julian oscillation. *J. Clim.* **27**, (2014).
30. Vellinga, M. & Milton, S. F. Drivers of interannual variability of the East African “Long Rains”. *Q. J. R. Meteorol. Soc.* **144**, (2018).
31. Martin, Z. *et al.* The influence of the quasi-biennial oscillation on the Madden–Julian oscillation. *Nature Reviews Earth and Environment* vol. 2 (2021).
32. Gelaro, R. *et al.* The modern-era retrospective analysis for research and applications, version 2 (MERRA-2). *J. Clim.* **30**, 5419–5454 (2017).
33. Huesmann, A. S. & Hitchman, M. H. The stratospheric quasi-biennial oscillation in the NCEP reanalyses: Climatological structures. *J. Geophys. Res. Atmos.* **106**, (2001).
34. Indeje, M. & Semazzi, F. H. M. Relationships between QBO in the lower equatorial stratospheric zonal winds and East African seasonal rainfall. *Meteorol. Atmos. Phys.* **73**, (2000).
35. Liu, W., Cook, K. H. & Vizzy, E. K. Influence of Indian Ocean SST regionality on the East African short rains. *Clim. Dyn.* **54**, (2020).
36. Dyer, E. & Washington, R. Kenyan long rains: A subseasonal approach to process-based diagnostics. *J. Clim.* **34**, (2021).
37. Kilavi, M. *et al.* Extreme Rainfall and Flooding over Central Kenya Including Nairobi City during the Long-Rains Season 2018: Causes, Predictability, and Potential for Early Warning and Actions. *Atmosphere (Basel)*. **9**, 472 (2018).
38. Kebacho, L. L. The Role of Tropical Cyclones Idai and Kenneth in Modulating Rainfall Performance of 2019 Long Rains over East Africa. *Pure Appl. Geophys.* (2022) doi:10.1007/s00024-022-02993-2.
39. Kebacho, L. L. Interannual variations of the monthly rainfall anomalies over Tanzania from March to May and their associated atmospheric circulations anomalies. *Nat. Hazards* (2022).
40. Tarnavsky, E. *et al.* Extension of the TAMSAT satellite-based rainfall monitoring over Africa and from 1983 to present. *J. Appl. Meteorol. Climatol.* **53**, (2014).
41. Maidment, R. I. *et al.* A new, long-term daily satellite-based rainfall dataset for operational monitoring in Africa. *Sci. Data* **4**, (2017).
42. Dai, A. Hydroclimatic trends during 1950–2018 over global land. *Clim. Dyn.* **56**, (2021).
43. Maidment, R. I., Allan, R. P. & Black, E. Recent observed and simulated changes in precipitation over Africa. *Geophys. Res. Lett.* **42**, (2015).
44. Cattani, E., Merino, A., Guijarro, J. A. & Levizzani, V. East Africa Rainfall trends and variability 1983-2015 using three long-term satellite products. *Remote Sens.* **10**, (2018).
45. Maidment, R. I. *et al.* The 30 year TAMSAT african rainfall climatology and time series (TARCAT) data set. *J. Geophys. Res.* **119**, (2014).
46. Liebmann, B. *et al.* Climatology and interannual variability of boreal spring wet season precipitation in the eastern horn of Africa and implications for its recent decline. *J. Clim.* **30**, 3867–3886 (2017).
47. Wainwright, C. M. *et al.* Eastern African Paradox rainfall decline due to shorter not less intense Long Rains. *npj Clim. Atmos. Sci.* **2**, (2019).
48. Walker, D. P., Marsham, J. H., Birch, C. E., Scaife, A. A. & Finney, D. L. Common Mechanism for Interannual and Decadal Variability in the East African Long Rains.



- Geophys. Res. Lett.* **47**, (2020).
49. Nicholson, S. E. Climate and climatic variability of rainfall over eastern Africa. *Rev. Geophys.* **55**, (2017).
  50. Tierney, J. E., Ummenhofer, C. C. & deMenocal, P. B. Past and future rainfall in the Horn of Africa. *Sci. Adv.* **1**, e1500682 (2015).
  51. Saji, N. H., Goswami, B. N., Vinayachandran, P. N. & Yamagata, T. A dipole mode in the tropical Indian Ocean. *Nature* **401**, 360–363 (1999).
  52. Webster, P. J., Moore, A. M., Loschnigg, J. P. & Leben, R. R. Coupled ocean-atmosphere dynamics in the Indian Ocean during 1997-98. *Nature* **401**, (1999).
  53. Funk, C. *et al.* Examining the potential contributions of extreme 'western v' sea surface temperatures to the 2017 March-June east african drought. *Bull. Am. Meteorol. Soc.* **100**, (2019).
  54. Liebmann, B. *et al.* Climatology and interannual variability of boreal spring wet season precipitation in the eastern horn of Africa and implications for its recent decline. *J. Clim.* **30**, (2017).
  55. Thielke, A. & Mölg, T. Observed and simulated Indian Ocean Dipole activity since the mid-19th century and its relation to East African short rains. *Int. J. Climatol.* **39**, (2019).
  56. Trenberth, K. E., Fasullo, J. T., Branstator, G. & Phillips, A. S. Seasonal aspects of the recent pause in surface warming. *Nat. Clim. Chang.* **4**, (2014).
  57. L'Heureux, M. L., Lee, S. & Lyon, B. Recent multidecadal strengthening of the Walker circulation across the tropical Pacific. *Nat. Clim. Chang.* **3**, (2013).
  58. England, M. H. *et al.* Recent intensification of wind-driven circulation in the Pacific and the ongoing warming hiatus. *Nat. Clim. Chang.* **4**, (2014).
  59. Seager, R. *et al.* Strengthening tropical Pacific zonal sea surface temperature gradient consistent with rising greenhouse gases. *Nature Climate Change* vol. 9 (2019).
  60. Black, E. The relationship between Indian Ocean sea-surface temperature and East African rainfall. *Philos. Trans. R. Soc. A Math. Phys. Eng. Sci.* **363**, (2005).
  61. Lyon, B. Seasonal drought in the Greater Horn of Africa and its recent increase during the March-May long rains. *J. Clim.* **27**, (2014).
  62. Allan, R. P. *et al.* Advances in understanding large-scale responses of the water cycle to climate change. *Annals of the New York Academy of Sciences* vol. 1472 (2020).
  63. Bronnimann, S. *et al.* Southward shift of the northern tropical belt from 1945 to 1980. *Nat. Geosci.* **8**, (2015).
  64. Undorf, S. *et al.* Detectable Impact of Local and Remote Anthropogenic Aerosols on the 20th Century Changes of West African and South Asian Monsoon Precipitation. *J. Geophys. Res. Atmos.* **123**, (2018).
  65. Dong, B. & Sutton, R. Dominant role of greenhouse-gas forcing in the recovery of Sahel rainfall. *Nat. Clim. Chang.* **5**, (2015).
  66. Blau, M. T. & Ha, K. J. The Indian Ocean Dipole and its Impact on East African Short Rains in Two CMIP5 Historical Scenarios With and Without Anthropogenic Influence. *J. Geophys. Res. Atmos.* **125**, (2020).
  67. Kew, S. F. *et al.* Impact of precipitation and increasing temperatures on drought trends in eastern Africa. *Earth Syst. Dyn.* **12**, (2021).
  68. Held, I. M. & Soden, B. J. Robust responses of the hydrological cycle to global warming. *J. Clim.* **19**, (2006).
  69. Vecchi, G. A. & Soden, B. J. Global warming and the weakening of the tropical circulation. *J. Clim.* **20**, (2007).
  70. Byrne, M. P. & Schneider, T. Narrowing of the ITCZ in a warming climate: Physical mechanisms. *Geophys. Res. Lett.* **43**, (2016).
  71. Byrne, M. P., Pendergrass, A. G., Rapp, A. D. & Wodzicki, K. R. Response of the Intertropical Convergence Zone to Climate Change: Location, Width, and Strength. *Current Climate Change Reports* vol. 4 (2018).
  72. Ayana, E. K., Ceccato, P., Fisher, J. R. B. & DeFries, R. Examining the relationship



- between environmental factors and conflict in pastoralist areas of East Africa. *Sci. Total Environ.* **557–558**, (2016).
73. Nakawuka, P., Langan, S., Schmitter, P. & Barron, J. A review of trends, constraints and opportunities of smallholder irrigation in East Africa. *Glob. Food Sec.* **17**, 196–212 (2018).
  74. Alter, R. E., Im, E. S. & Eltahir, E. A. B. Rainfall consistently enhanced around the Gezira Scheme in East Africa due to irrigation. *Nat. Geosci.* **8**, (2015).
  75. Vicente-Serrano, S. M. *et al.* Challenges for drought mitigation in Africa: The potential use of geospatial data and drought information systems. *Appl. Geogr.* **34**, (2012).
  76. Mera, G. A. Drought and its impacts in Ethiopia. *Weather Clim. Extrem.* **22**, 24–35 (2018).
  77. Funk, C. Ethiopia, Somalia and Kenya face devastating drought. *Nature* **586**, 645 (2020).
  78. Korecha, D. & Barnston, A. G. Predictability of June–September rainfall in Ethiopia. *Mon. Weather Rev.* **135**, (2007).
  79. Bachewe, F. N., Yimer, F., Minten, B. & Dorosh, P. A. *Agricultural prices during drought in Ethiopia. ESSP Working Paper* vol. 97 (2016).
  80. Obasi, G. O. P. The impacts of ENSO in Africa. in *Climate Change and Africa* vol. 9780521836340 (2005).
  81. Desta, Z. H. & Oba, G. Feed scarcity and livestock mortality in enset farming systems in the Bale highlands of southern Ethiopia. *Outlook Agric.* **33**, (2004).
  82. Habte, M., Eshetu, M., Maryo, M., Andualem, D. & Legesse, A. Effects of climate variability on livestock productivity and pastoralists perception: The case of drought resilience in Southeastern Ethiopia. *Vet. Anim. Sci.* **16**, (2022).
  83. Funk, C. *et al.* Recognizing the famine early warning systems network over 30 years of drought early warning science advances and partnerships promoting global food security. *Bull. Am. Meteorol. Soc.* **100**, (2019).
  84. Novella, N. S. & Thiaw, W. M. African rainfall climatology version 2 for famine early warning systems. *J. Appl. Meteorol. Climatol.* **52**, 588–606 (2013).
  85. Backer, D. & Billing, T. Validating Famine Early Warning Systems Network projections of food security in Africa, 2009–2020. *Glob. Food Sec.* **29**, (2021).
  86. Simtowe, F. *et al.* Heterogeneous seed access and information exposure: implications for the adoption of drought-tolerant maize varieties in Uganda. *Agric. Food Econ.* **7**, (2019).
  87. Philip, S. *et al.* The drought in Ethiopia, 2015. *Clim. Dev. Knowl. Netw. World Weather Attrib. Initiat.* (2017).
  88. Toret, A. *et al.* *Drought in East Africa August 2022*. (2022).
  89. Yang, M. *et al.* The role of climate in the trend and variability of Ethiopia's cereal crop yields. *Sci. Total Environ.* **723**, 137893 (2020).
  90. Wilkes, M. A. *et al.* Physical and biological controls on fine sediment transport and storage in rivers. *Wiley Interdisciplinary Reviews: Water* vol. 6 (2019).
  91. Gebrehiwot, K. A. A review on waterlogging, salinization and drainage in Ethiopian irrigated agriculture. *Sustain. Water Resour. Manag.* **4**, 55–62 (2018).
  92. Fenta, A. A. *et al.* Cropland expansion outweighs the monetary effect of declining natural vegetation on ecosystem services in sub-Saharan Africa. *Ecosyst. Serv.* **45**, 101154 (2020).
  93. Showler, A. T. Locust 1 (Orthoptera: Acrididae) Outbreak in Africa and Asia, 1992–1994: An Overview. *Am. Entomol.* (1995) doi:10.1093/ae/41.3.179.
  94. Foster, Z. J. The 1915 Locust Attack in Syria and Palestine and its Role in the Famine During the First World War. *Middle East. Stud.* (2015) doi:10.1080/00263206.2014.976624.
  95. Showler, A. T. & Potter, C. S. Synopsis of the 1986–1989 Desert Locust (Orthoptera: Acrididae) Plague and the Concept of Strategic Control. *Am. Entomol.* **37**, (1991).
  96. Bennett, L. V. The development and termination of the 1968 plague of the desert locust, *Schistocerca gregaria* (Forskål) (Orthoptera, Acrididae). *Bull. Entomol. Res.*

- 66, (1976).
97. Showler, A. T. & Lecoq, M. Incidence and ramifications of armed conflict in countries with major desert locust breeding areas. *Agronomy* (2021) doi:10.3390/AGRONOMY11010114.
98. IPC. IPC Alert on Locusts by The Integrated Food Security Phase Classification. (2020).
99. Kray, H. & Shetty, S. The locust plague: Fighting a crisis within a crisis. (2020).
100. FAO. *Impact of Desert Locust Infestation on Household Livelihoods and Food Security in Ethiopia: Joint Assessment Findings*. (2020).
101. Singh, V. K. & Roxy, M. K. A review of ocean-atmosphere interactions during tropical cyclones in the north Indian Ocean. *Earth-Science Reviews* vol. 226 (2022).
102. Yuan, J. P. & Cao, J. North Indian Ocean tropical cyclone activities influenced by the Indian Ocean Dipole mode. *Sci. China Earth Sci.* **56**, (2013).
103. Madani, N. *et al.* Below-surface water mediates the response of African forests to reduced rainfall. *Environ. Res. Lett.* **15**, (2020).
104. Guan, K. *et al.* Photosynthetic seasonality of global tropical forests constrained by hydroclimate. *Nat. Geosci.* **8**, (2015).
105. Madani, N., Kimball, J. S., Jones, L. A., Parazoo, N. C. & Guan, K. Global analysis of bioclimatic controls on ecosystem productivity using satellite observations of solar-induced chlorophyll fluorescence. *Remote Sens.* **9**, (2017).
106. Schenk, H. J. & Jackson, R. B. Rooting depths, lateral root spreads and below-ground/above-ground allometries of plants in water-limited ecosystems. *J. Ecol.* **90**, (2002).
107. Jones, L. A. *et al.* The SMAP Level 4 Carbon Product for Monitoring Ecosystem Land-Atmosphere CO<sub>2</sub> Exchange. *IEEE Trans. Geosci. Remote Sens.* **55**, (2017).
108. Bauer, S. E., Im, U., Mezuman, K. & Gao, C. Y. Desert Dust, Industrialization, and Agricultural Fires: Health Impacts of Outdoor Air Pollution in Africa. *J. Geophys. Res. Atmos.* **124**, (2019).
109. Jaeglé, L., Steinberger, L., Martin, R. V. & Chance, K. Global partitioning of NO<sub>x</sub> sources using satellite observations: Relative roles of fossil fuel combustion, biomass burning and soil emissions. in *Faraday Discussions* vol. 130 (2005).
110. van der Werf, G. R. *et al.* Global fire emissions estimates during 1997–2016. *Earth Syst. Sci. Data* **9**, 697–720 (2017).
111. Bistinas, I., Harrison, S. P., Prentice, I. C. & Pereira, J. M. C. Causal relationships versus emergent patterns in the global controls of fire frequency. *Biogeosciences* **11**, (2014).
112. Finney, D. L. *et al.* African Lightning and its Relation to Rainfall and Climate Change in a Convection-Permitting Model. *Geophys. Res. Lett.* **47**, (2020).
113. Andela, N. *et al.* A human-driven decline in global burned area. *Science* (80-. ). **356**, (2017).
114. Andela, N. & Van Der Werf, G. R. Recent trends in African fires driven by cropland expansion and El Niño to la Niña transition. *Nat. Clim. Chang.* **4**, (2014).
115. Chen, Y. *et al.* A pan-tropical cascade of fire driven by El Niño/Southern Oscillation. *Nat. Clim. Chang.* **7**, (2017).
116. Kim, I. W. *et al.* Tropical Indo-Pacific SST influences on vegetation variability in eastern Africa. *Sci. Rep.* **11**, (2021).
117. Ringeval, B. *et al.* An attempt to quantify the impact of changes in wetland extent on methane emissions on the seasonal and interannual time scales. *Global Biogeochem. Cycles* (2010) doi:10.1029/2008GB003354.
118. Bloom, A. A., Palmer, P. I., Fraser, A., David, S. R. & Frankenberg, C. Large-scale controls of methanogenesis inferred from methane and gravity spaceborne data. *Science* (80-. ). (2010) doi:10.1126/science.1175176.
119. Whalen, S. C. Biogeochemistry of methane exchange between natural wetlands and the atmosphere. *Environmental Engineering Science* (2005) doi:10.1089/ees.2005.22.73.

120. Bloom, A. A., Palmer, P. I., Fraser, A., Reay, D. S. & Frankenberg, C. Large-Scale Controls of Methanogenesis Inferred from Methane and Gravity Spaceborne Data. *Science* (80-. ). **327**, 322–325 (2010).
121. Helfter, C. *et al.* Phenology is the dominant control of methane emissions in a tropical non-forested wetland. *Nat. Commun.* **13**, 133 (2022).
122. Joabsson, A., Christensen, T. R. & Wallén, B. Vascular plant controls on methane emissions from northern peatforming wetlands. *Trends in Ecology and Evolution* (1999) doi:10.1016/S0169-5347(99)01649-3.
123. Dingemans, B. J. J., Barker, E. S. & Bodelier, P. L. E. Aquatic herbivores facilitate the emission of methane from wetlands. *Ecology* (2011) doi:10.1890/10-1297.1.
124. Lunt, M. F. *et al.* An increase in methane emissions from tropical Africa between 2010 and 2016 inferred from satellite data. *Atmos. Chem. Phys.* **19**, 14721–14740 (2019).
125. Lunt, M. F. *et al.* Rain-fed pulses of methane from East Africa during 2018-2019 contributed to atmospheric growth rate. *Environ. Res. Lett.* **16**, 24021 (2021).
126. Pandey, S. *et al.* Using satellite data to identify the methane emission controls of South Sudan's wetlands. *Biogeosciences* (2021) doi:10.5194/bg-18-557-2021.
127. Feng, L., Palmer, P. I., Zhu, S., Parker, R. J. & Liu, Y. Tropical methane emissions explain large fraction of recent changes in global atmospheric methane growth rate. *Nat. Commun.* **13**, 1378 (2022).
128. Sutcliffe, J. V. & Parks, Y. P. *The hydrology of the Nile. The hydrology of the Nile. IAHS Special Publication No.5.* (1999).
129. Sutcliffe, J. & Brown, E. Water losses from the Sudd. *Hydrol. Sci. J.* (2018) doi:10.1080/02626667.2018.1438612.
130. Lunt, M. F. *et al.* Rain-fed pulses of methane from East Africa during 2018-2019 contributed to atmospheric growth rate. *Environ. Res. Lett.* **16**, 24021 (2021).
131. Qu, Z. *et al.* Attribution of the 2020 surge in atmospheric methane by inverse analysis of GOSAT observations. *Environ. Res. Lett.* **17**, 094003 (2022).
132. Feng, L., Palmer, P. I., Parker, R. J., Lunt, M. F. & Boesch, H. Methane emissions responsible for record-breaking atmospheric methane growth rates in 2020 and 2021. *Atmos. Chem. Phys. Discuss.* **2022**, 1–23 (2022).
133. Van Damme, M. *et al.* Industrial and agricultural ammonia point sources exposed. *Nature* **564**, (2018).
134. Dammers, E. *et al.* NH<sub>3</sub> emissions from large point sources derived from CrIS and IASI satellite observations. *Atmos. Chem. Phys.* **19**, (2019).
135. Bauer, S. E., Tsigaridis, K. & Miller, R. Significant atmospheric aerosol pollution caused by world food cultivation. *Geophys. Res. Lett.* **43**, (2016).
136. Lelieveld, J., Evans, J. S., Fnais, M., Giannadaki, D. & Pozzer, A. The contribution of outdoor air pollution sources to premature mortality on a global scale. *Nature* **525**, (2015).
137. Denier Van Der Gon, H. & Bleeker, A. Indirect N<sub>2</sub>O emission due to atmospheric N deposition for the Netherlands. *Atmos. Environ.* **39**, (2005).
138. Krupa, S. V. Effects of atmospheric ammonia (NH<sub>3</sub>) on terrestrial vegetation: A review. *Environmental Pollution* vol. 124 (2003).
139. Matson, P. A., McDowell, W. H., Townsend, A. R. & Vitousek, P. M. The globalization of N deposition: Ecosystem consequences in tropical environments. *Biogeochemistry* **46**, (1999).
140. Tian, D. & Niu, S. A global analysis of soil acidification caused by nitrogen addition. *Environ. Res. Lett.* **10**, (2015).
141. Koutsoyiannis, D., Yao, H. & Georgakakos, A. Medium-range flow prediction for the Nile: a comparison of stochastic and deterministic methods / Prévision du débit du Nil à moyen terme: une comparaison de méthodes stochastiques et déterministes. *Hydrol. Sci. J.* **53**, 142–164 (2008).
142. Kim, M. & Or, D. Microscale pH variations during drying of soils and desert biocrusts affect HONO and NH<sub>3</sub> emissions. *Nat. Commun.* **10**, (2019).
143. Roelle, P. A. & Aneja, V. P. Characterization of ammonia emissions from soils in the

- upper coastal plain, North Carolina. *Atmos. Environ.* **36**, (2002).
144. Clarisse, L. *et al.* Atmospheric ammonia (NH<sub>3</sub>) emanations from Lake Natron's saline mudflats. *Sci. Rep.* **9**, (2019).
  145. Hickman, J. E. *et al.* Changes in biomass burning, wetland extent, or agriculture drive atmospheric NH<sub>3</sub> trends in select African regions. *Atmos. Chem. Phys.* **21**, (2021).
  146. Di Vittorio, C. A. & Georgakakos, A. P. Land cover classification and wetland inundation mapping using MODIS. *Remote Sens. Environ.* **204**, (2018).
  147. Oluwasanya, G. . P. D. . Q. M. . S. V. *Water Security in Africa: A Preliminary Assessment* . (2022).
  148. Sridharan, V. *et al.* Resilience of the Eastern African electricity sector to climate driven changes in hydropower generation. *Nat. Commun.* **10**, 302 (2019).
  149. Jeuland, M. Economic implications of climate change for infrastructure planning in transboundary water systems: An example from the Blue Nile. *Water Resour. Res.* **46**, W11556 (2010).
  150. Jeuland, M. & Whittington, D. Water resources planning under climate change: Assessing the robustness of real options for the Blue Nile. *Water Resour. Res.* **50**, 2086–2107 (2014).
  151. Conway, D. Water resources: Future Nile river flows. *Nat. Clim. Chang.* **7**, 319–320 (2017).
  152. Siderius, C. *et al.* Hydrological Response and Complex Impact Pathways of the 2015/2016 El Niño in Eastern and Southern Africa. *Earth's Futur.* **6**, (2018).
  153. Samboko, P. *et al.* The Impact of Power Rationing on Zambia's Agricultural Sector. *Work. Pap. No. 105* (2016).
  154. Dinar, A., Blankespoor, B., Dinar, S. & Kurukulasuriya, P. Does precipitation and runoff variability affect treaty cooperation between states sharing international bilateral rivers? *Ecol. Econ.* **69**, 2568–2581 (2010).
  155. Wheeler, K. G., Jeuland, M., Hall, J. W., Zagana, E. & Whittington, D. Understanding and managing new risks on the Nile with the Grand Ethiopian Renaissance Dam. *Nat. Commun.* **11**, 5222 (2020).
  156. Peña-Ramos, J. A., José López-Bedmar, R., Sastre, F. J. & Martínez-Martínez, A. Water Conflicts in Sub-Saharan Africa. *Front. Environ. Sci.* **10**, (2022).
  157. Wolf, A. T. Shared Waters: Conflict and Cooperation. *Annu. Rev. Environ. Resour.* **32**, 241–269 (2007).
  158. Wheeler, K. G. *et al.* Cooperative filling approaches for the Grand Ethiopian Renaissance Dam. *Water Int.* **41**, 611–634 (2016).
  159. Calderón, C. & Servén, L. Infrastructure and Economic Development in Sub-Saharan Africa †. *J. Afr. Econ.* **19**, i13–i87 (2010).
  160. Douglas, I. *et al.* Unjust waters: climate change, flooding and the urban poor in Africa. *Environ. Urban.* **20**, 187–205 (2008).
  161. Birhanu, D., Kim, H., Jang, C. & Park, S. Flood Risk and Vulnerability of Addis Ababa City Due to Climate Change and Urbanization. *Procedia Eng.* **154**, 696–702 (2016).
  162. Mahmood, M. I., Elagib, N. A., Horn, F. & Saad, S. A. G. Lessons learned from Khartoum flash flood impacts: An integrated assessment. *Sci. Total Environ.* **601–602**, 1031–1045 (2017).
  163. AFB. Flooding: Sudan. *Africa Res. Bull. Econ. Financ. Tech. Ser.* **57**, 23103A-23106C (2020).
  164. Thomson, M. C., Muñoz, Á. G., Cousin, R. & Shumake-Guillemot, J. Climate drivers of vector-borne diseases in Africa and their relevance to control programmes. *Infect. Dis. Poverty* (2018) doi:10.1186/s40249-018-0460-1.
  165. Caminade, C., McIntyre, K. M. & Jones, A. E. Impact of recent and future climate change on vector-borne diseases. *Annals of the New York Academy of Sciences* (2019) doi:10.1111/nyas.13950.
  166. Endo, N. & Eltahir, E. A. B. Increased risk of malaria transmission with warming temperature in the Ethiopian Highlands. *Environ. Res. Lett.* **15**, 54006 (2020).
  167. Brown, V., Issak, M. A., Rossi, M., Barboza, P. & Paugam, A. Epidemic of malaria in



- north-eastern Kenya. *Lancet* (1998) doi:10.1016/S0140-6736(05)60747-7.
168. Kilian, A. H. D., Langi, P., Talisuna, A. & Kabagambe, G. Rainfall pattern, El Nino and malaria in Uganda. *Trans. R. Soc. Trop. Med. Hyg.* (1999) doi:10.1016/S0035-9203(99)90165-7.
  169. Boyce, R. *et al.* Severe Flooding and Malaria Transmission in the Western Ugandan Highlands: Implications for Disease Control in an Era of Global Climate Change. *J. Infect. Dis.* (2016) doi:10.1093/infdis/jiw363.
  170. Nosrat, C. *et al.* Impact of recent climate extremes on mosquito-borne disease transmission in Kenya. *PLoS Negl. Trop. Dis.* (2021) doi:10.1371/journal.pntd.0009182.
  171. Hashizume, M., Terao, T. & Minakawa, N. The Indian Ocean Dipole and malaria risk in the highlands of western Kenya. *Proc. Natl. Acad. Sci. U. S. A.* (2009) doi:10.1073/pnas.0806544106.
  172. Hashizume, M., Chaves, L. F. & Minakawa, N. Indian Ocean Dipole drives malaria resurgence in East African highlands. *Sci. Rep.* (2012) doi:10.1038/srep00269.
  173. Moore, S. M. *et al.* El Niño and the shifting geography of cholera in Africa. *Proc. Natl. Acad. Sci. U. S. A.* (2017) doi:10.1073/pnas.1617218114.
  174. Rieckmann, A., Tamason, C. C., Gurley, E. S., Rod, N. H. & Jensen, P. K. M. Exploring droughts and floods and their association with cholera outbreaks in sub-Saharan Africa: a register-based ecological study from 1990 to 2010. *Am. J. Trop. Med. Hyg.* (2018) doi:10.4269/ajtmh.17-0778.
  175. Lindsay, S. W., Bødker, R., Malima, R., Msangeni, H. A. & Kisinza, W. Effect of 1997-98 El Niño on highland malaria in Tanzania. *Lancet* (2000) doi:10.1016/S0140-6736(00)90022-9.
  176. Chemura, A., Mudereri, B. T., Yalew, A. W. & Gornott, C. Climate change and specialty coffee potential in Ethiopia. *Sci. Rep.* **11**, (2021).
  177. Lobell, D. B. & Burke, M. B. Why are agricultural impacts of climate change so uncertain? the importance of temperature relative to precipitation. *Environ. Res. Lett.* **3**, (2008).
  178. Tigchelaar, M., Battisti, D. S., Naylor, R. L. & Ray, D. K. Future warming increases probability of globally synchronized maize production shocks. *Proc. Natl. Acad. Sci. U. S. A.* **115**, (2018).
  179. Shapiro, L. L. M., Whitehead, S. A. & Thomas, M. B. Quantifying the effects of temperature on mosquito and parasite traits that determine the transmission potential of human malaria. *PLoS Biol.* **15**, (2017).
  180. Yang, W., Seager, R., Cane, M. A. & Lyon, B. The East African long rains in observations and models. *J. Clim.* **27**, (2014).
  181. Rowell, D. P., Booth, B. B. B., Nicholson, S. E. & Good, P. Reconciling past and future rainfall trends over East Africa. *J. Clim.* **28**, (2015).
  182. Dunning, C. M., Black, E. & Allan, R. P. Later Wet Seasons with More Intense Rainfall over Africa under Future Climate Change. *J. Clim.* **31**, 9719–9738 (2018).
  183. Makula, E. K. & Zhou, B. Coupled Model Intercomparison Project phase 6 evaluation and projection of East African precipitation. *Int. J. Climatol.* (2021) doi:10.1002/joc.7373.
  184. Cook, B. I. *et al.* Twenty-First Century Drought Projections in the CMIP6 Forcing Scenarios. *Earth's Futur.* **8**, (2020).
  185. Ongoma, V., Chena, H. & Gao, C. Projected changes in mean rainfall and temperature over East Africa based on CMIP5 models. *Int. J. Climatol.* **38**, (2018).
  186. Akinsanola, A. A., Ongoma, V. & Kooperman, G. J. Evaluation of CMIP6 models in simulating the statistics of extreme precipitation over Eastern Africa. *Atmos. Res.* **254**, (2021).
  187. Rowell, D. P., Senior, C. A., Vellinga, M. & Graham, R. J. Can climate projection uncertainty be constrained over Africa using metrics of contemporary performance? *Clim. Change* **134**, (2016).
  188. Endris, H. S. *et al.* Future changes in rainfall associated with ENSO, IOD and



- changes in the mean state over Eastern Africa. *Clim. Dyn.* **52**, (2019).
189. Ayugi, B. *et al.* Comparison of CMIP6 and CMIP5 models in simulating mean and extreme precipitation over East Africa. *Int. J. Climatol.* **41**, (2021).
  190. Iturbide, M. *et al.* Repository supporting the implementation of FAIR principles in the IPCC-WG1 Atlas. (2021) doi:10.5281/zenodo.3691645.
  191. Finney, D. L. *et al.* Effects of Explicit Convection on Future Projections of Mesoscale Circulations, Rainfall, and Rainfall Extremes over Eastern Africa. *J. Clim.* **33**, 2701–2718 (2020).
  192. Lyon, B. Biases in sea surface temperature and the annual cycle of Greater Horn of Africa rainfall in CMIP6. *Int. J. Climatol.* (2021) doi:10.1002/joc.7456.
  193. King, J. A., Washington, R. & Engelstaedter, S. Representation of the Indian Ocean Walker circulation in climate models and links to Kenyan rainfall. *Int. J. Climatol.* **41**, (2021).
  194. Cai, W. *et al.* Changing El Niño–Southern Oscillation in a warming climate. *Nature Reviews Earth and Environment* vol. 2 (2021).
  195. Zelle, H., van Oldenborgh, G. J., Burgers, G. & Dijkstra, H. El Niño and greenhouse warming: Results from ensemble simulations with the NCAR CCSM. *J. Clim.* **18**, (2005).
  196. Merryfield, W. J. Changes to ENSO under CO<sub>2</sub> doubling in a multimodel ensemble. *J. Clim.* **19**, (2006).
  197. Collins, M. *et al.* The impact of global warming on the tropical Pacific Ocean and El Niño. *Nat. Geosci.* **3**, (2010).
  198. Cai, W. *et al.* Increasing frequency of extreme El Niño events due to greenhouse warming. *Nat. Clim. Chang.* **4**, (2014).
  199. Cai, W. *et al.* ENSO and greenhouse warming. *Nature Climate Change* vol. 5 (2015).
  200. Singh, J. *et al.* Enhanced risk of concurrent regional droughts with increased ENSO variability and warming. *Nat. Clim. Chang.* **12**, 163–170 (2022).
  201. Zheng, X. T. *et al.* Indian ocean dipole response to global warming in the CMIP5 multimodel ensemble. *J. Clim.* **26**, (2013).
  202. Cai, W. & Cowan, T. Why is the amplitude of the Indian ocean dipole overly large in CMIP3 and CMIP5 climate models? *Geophys. Res. Lett.* **40**, (2013).
  203. Cai, W. *et al.* Opposite response of strong and moderate positive Indian Ocean Dipole to global warming. *Nat. Clim. Chang.* **11**, (2021).
  204. Douville, H. *et al.* Climate Change 2021: The Physical Science Basis. Contribution of Working Group I to the Sixth Assessment Report of the Intergovernmental Panel on Climate Change. in (Cambridge University Press, 2021).
  205. Chu, J. E. *et al.* Future change of the Indian Ocean basin-wide and dipole modes in the CMIP5. *Clim. Dyn.* **43**, (2014).
  206. Mamalakos, A. *et al.* Zonally contrasting shifts of the tropical rain belt in response to climate change. *Nat. Clim. Chang.* **11**, (2021).
  207. Schlenker, W. & Roberts, M. J. Nonlinear temperature effects indicate severe damages to U.S. crop yields under climate change. *Proc. Natl. Acad. Sci. U. S. A.* **106**, (2009).
  208. Wang, X., Xie, H., Guan, H. & Zhou, X. Different responses of MODIS-derived NDVI to root-zone soil moisture in semi-arid and humid regions. *J. Hydrol.* **340**, (2007).
  209. Guido, Z. *et al.* Farmer forecasts: Impacts of seasonal rainfall expectations on agricultural decision-making in Sub-Saharan Africa. *Clim. Risk Manag.* **30**, (2020).
  210. Thornton, P. K., van de Steeg, J., Notenbaert, A. & Herrero, M. The impacts of climate change on livestock and livestock systems in developing countries: A review of what we know and what we need to know. *Agricultural Systems* vol. 101 (2009).
  211. Senande-Rivera, M., Insua-Costa, D. & Miguez-Macho, G. Spatial and temporal expansion of global wildland fire activity in response to climate change. *Nat. Commun.* **13**, 1208 (2022).
  212. Piao, S. *et al.* Characteristics, drivers and feedbacks of global greening. *Nature Reviews Earth and Environment* vol. 1 (2020).

213. Zarei, A., Chemura, A., Gleixner, S. & Hoff, H. Evaluating the grassland NPP dynamics in response to climate change in Tanzania. *Ecol. Indic.* **125**, (2021).
214. Martens, C. *et al.* Large uncertainties in future biome changes in Africa call for flexible climate adaptation strategies. *Glob. Chang. Biol.* **27**, (2021).
215. Doherty, R. M., Sitch, S., Smith, B., Lewis, S. L. & Thornton, P. K. Implications of future climate and atmospheric CO<sub>2</sub> content for regional biogeochemistry, biogeography and ecosystem services across East Africa. *Glob. Chang. Biol.* **16**, (2010).
216. Scheiter, S. & Higgins, S. I. Impacts of climate change on the vegetation of Africa: An adaptive dynamic vegetation modelling approach. *Glob. Chang. Biol.* **15**, (2009).
217. Kim, J. H. *et al.* A Systematic Review of Typhoid Fever Occurrence in Africa. *Clinical Infectious Diseases* vol. 69 (2019).
218. Lahondre, C. & Lazzari, C. R. Mosquitoes cool down during blood feeding to avoid overheating. *Curr. Biol.* **22**, (2012).
219. Colón-González, F. J. *et al.* Projecting the risk of mosquito-borne diseases in a warmer and more populated world: a multi-model, multi-scenario intercomparison modelling study. *Lancet Planet. Heal.* **5**, (2021).
220. Ryan, S. J., Lippi, C. A. & Zermoglio, F. Shifting transmission risk for malaria in Africa with climate change: A framework for planning and intervention. *Malar. J.* **19**, (2020).
221. Kolstad, E. W., MacLeod, D. & Demissie, T. D. Drivers of Subseasonal Forecast Errors of the East African Short Rains. *Geophys. Res. Lett.* **48**, (2021).
222. Ogutu, G. E. O., Franssen, W. H. P., Supit, I., Omondi, P. & Hutjes, R. W. A. Skill of ECMWF system-4 ensemble seasonal climate forecasts for East Africa. *Int. J. Climatol.* **37**, (2017).
223. Young, H. R. & Klingaman, N. P. Skill of seasonal rainfall and temperature forecasts for East Africa. *Weather Forecast.* **35**, (2020).
224. Funk, C. *et al.* Predicting East African spring droughts using Pacific and Indian Ocean sea surface temperature indices. *Hydrol. Earth Syst. Sci.* **18**, (2014).
225. Mutai, C. C., Ward, M. N. & Colman, A. W. Towards the prediction of the East Africa short rains based on sea-surface temperature-atmosphere coupling. *Int. J. Climatol.* **18**, (1998).
226. Nicholson, S. E. The predictability of rainfall over the greater horn of Africa. Part I: Prediction of seasonal rainfall. *J. Hydrometeorol.* **15**, (2014).
227. Meehl, G. A. *et al.* Initialized Earth System prediction from subseasonal to decadal timescales. *Nature Reviews Earth and Environment* vol. 2 (2021).
228. MacLeod, D. Seasonal forecasts of the East African long rains: insight from atmospheric relaxation experiments. *Clim. Dyn.* **53**, (2019).
229. Phillips, H. E. *et al.* Progress in understanding of Indian Ocean circulation, variability, air-sea exchange, and impacts on biogeochemistry. *Ocean Science* vol. 17 (2021).
230. Majumdar, S. J. A review of targeted observations. *Bulletin of the American Meteorological Society* vol. 97 (2016).
231. Dong, B., Haines, K. & Martin, M. Improved High Resolution Ocean Reanalyses Using a Simple Smoother Algorithm. *J. Adv. Model. Earth Syst.* **13**, (2021).
232. Nordling, L. Scientists struggle to access Africa's historical climate data. *Nature* vol. 574 (2019).
233. Smith, M. J. *et al.* Changing how earth system modeling is done to provide more useful information for decision making, science, and society. *Bulletin of the American Meteorological Society* vol. 95 (2014).
234. Webster, P. J. Meteorology: Improve weather forecasts for the developing world. *Nature* vol. 493 (2013).
235. Mordecai, E. A., Ryan, S. J., Caldwell, J. M., Shah, M. M. & LaBeaud, A. D. Climate change could shift disease burden from malaria to arboviruses in Africa. *Lancet Planet. Heal.* **4**, e416–e423 (2020).
236. Allen, T. *et al.* Global hotspots and correlates of emerging zoonotic diseases. *Nat. Commun.* **8**, (2017).

237. Lipp, E. K., Huq, A. & Colwell, R. R. Effects of global climate on infectious disease: The cholera model. *Clinical Microbiology Reviews* vol. 15 (2002).
238. Tamerius, J. D. *et al.* Environmental Predictors of Seasonal Influenza Epidemics across Temperate and Tropical Climates. *PLoS Pathog.* **9**, (2013).
239. Palmer, P. I. *et al.* Net carbon emissions from African biosphere dominate pan-tropical atmospheric CO<sub>2</sub> signal. *Nat. Commun.* **10**, 3344 (2019).
240. Merbold, L. *et al.* Opportunities for an African greenhouse gas observation system. *Reg. Environ. Chang.* **21**, (2021).
241. Wang, T. *et al.* Why is the Indo-Gangetic Plain the region with the largest NH<sub>3</sub> column in the globe during pre-monsoon and monsoon seasons? *Atmos. Chem. Phys.* **20**, 8727–8736 (2020).
242. Cai, W. *et al.* Projected response of the Indian Ocean Dipole to greenhouse warming. *Nature Geoscience* vol. 6 (2013).
243. Tramberend, S. *et al.* Co-development of East African regional water scenarios for 2050. *One Earth* **4**, (2021).
244. Zhao, G., Li, Y., Zhou, L. & Gao, H. Evaporative water loss of 1.42 million global lakes. *Nat. Commun.* **13**, 3686 (2022).
245. Haghighi, E., Madani, K. & Hoekstra, A. Y. The water footprint of water conservation using shade balls in California. *Nat. Sustain.* **1**, (2018).
246. FAO and UN Water. *Progress on change in water-use efficiency. Global status and acceleration needs for SDG indicator 6.4.1.* (2021).
247. Acreman, M. C. *et al.* Managed flood releases from reservoirs: issues and guidance. *Rep. to DFID World Comm. Dams. Cent. Ecol. Hydrol. Wallingford, UK* **2000**, p86 (2000).
248. Wang, J. *et al.* Exploitation of drought tolerance-related genes for crop improvement. *International Journal of Molecular Sciences* vol. 22 (2021).
249. Biamah, E. K., Gichuki, F. N. & Kaumbutho, P. G. Tillage methods and soil and water conservation in eastern Africa. *Soil Tillage Res.* **27**, (1993).
250. Parncutt, R. The human cost of anthropogenic global warming: Semi-quantitative prediction and the 1,000-tonne rule. *Front. Psychol.* **10**, (2019).
251. Schreck, C. J. & Semazzi, F. H. M. Variability of the recent climate of eastern Africa. *Int. J. Climatol.* **24**, 681–701 (2004).
252. Sutcliffe, J. & Parks, Y. *The hydrology of the Nile.* (IAHS Press, 1999).
253. Alsdorf, D. *et al.* Opportunities for hydrologic research in the Congo Basin. *Reviews of Geophysics* vol. 54 (2016).
254. Lehner, B. & Grill, G. Global river hydrography and network routing: Baseline data and new approaches to study the world's large river systems. *Hydrol. Process.* **27**, (2013).
255. Becker, A. *et al.* A description of the global land-surface precipitation data products of the Global Precipitation Climatology Centre with sample applications including centennial (trend) analysis from 1901-present. *Earth Syst. Sci. Data* **5**, (2013).
256. Schneider, U. *et al.* GPCC's new land surface precipitation climatology based on quality-controlled in situ data and its role in quantifying the global water cycle. *Theor. Appl. Climatol.* **115**, (2014).
257. Funk, C. *et al.* The climate hazards infrared precipitation with stations - A new environmental record for monitoring extremes. *Sci. Data* **2**, (2015).
258. Gedney, N., Huntingford, C., Comyn-Platt, E. & Wiltshire, A. Significant feedbacks of wetland methane release on climate change and the causes of their uncertainty. *Environ. Res. Lett.* **14**, (2019).
259. Best, M. J. *et al.* The Joint UK Land Environment Simulator (JULES), model description – Part 1: Energy and water fluxes. *Geosci. Model Dev.* **4**, (2011).
260. Clark, D. B. *et al.* The Joint UK Land Environment Simulator (JULES), model description – Part 2: Carbon fluxes and vegetation dynamics. *Geosci. Model Dev.* **4**, (2011).
261. Huntingford, C. *et al.* IMOGEN: An intermediate complexity model to evaluate terrestrial impacts of a changing climate. *Geosci. Model Dev.* **3**, (2010).

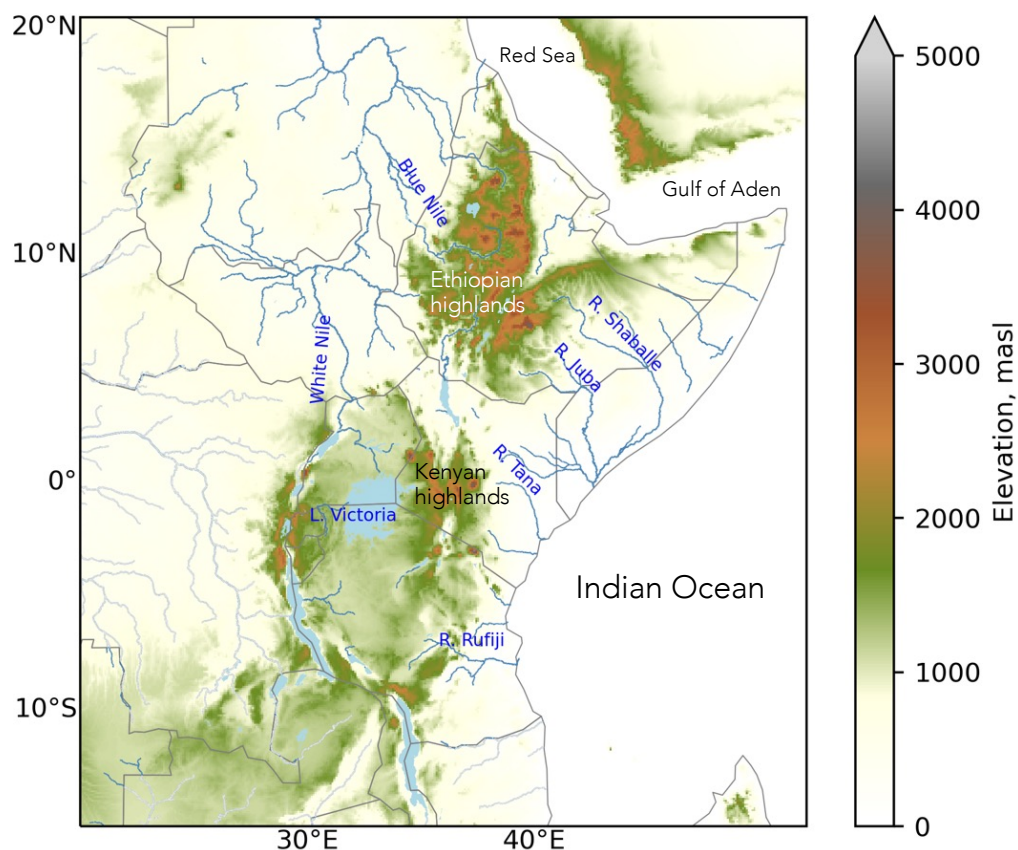
1589 262. Huntingford, C. & Cox, P. M. An analogue model to derive additional climate change  
1590 scenarios from existing GCM simulations. *Clim. Dyn.* **16**, (2000).  
1591  
1592  
1593

## BOX 1: Physical geography of Eastern Africa

The physical geography of Eastern Africa is relevant to the dynamics of rainfall weather systems<sup>49,251</sup> and to the subsequent surface movement of water (see figure). The region is dominated by the East African Rift, running from the Afar Triple Junction near the Red Sea southwards through Eastern Africa to Mozambique that also produces the Ethiopian and Kenyan Highlands.

Eastern Africa is dominated by the Nile River basin but also encompasses tributaries of the Congo as well several regionally important rivers draining eastwards into the Red Sea, the Gulf of Aden and the Indian Ocean. Two endorheic rivers, the Awash and Omo, terminate in the Afar depression and Lake Turkana, respectively. The Nile Basin includes several rift valley lakes including Lake Victoria which collects water from Burundi, Rwanda, northern Tanzania, and the Kenyan Highlands and has an important role in regulating flows in the White Nile downstream.

Tributaries draining the western Ethiopian highlands bring additional seasonal flows (during August-October) with the largest of these, the Blue Nile, joining at Khartoum to form the main river Nile<sup>252</sup>. Lake Kivu and Lake Tanganyika and its tributaries in western Tanzania form the headwaters of the Congo<sup>253</sup>. Watersheds east and south of the Ethiopian highlands and eastern rift valley flow into the Indian Ocean, providing an essential source of water to populations in more arid coastal plains, for example Shabelle and Juba in Somalia. In addition to the rift valley lakes, areas of extensive seasonal flooding, for example the Sudd in South Sudan, lead to significant water losses to the atmosphere by evaporation<sup>129</sup>.





Figure

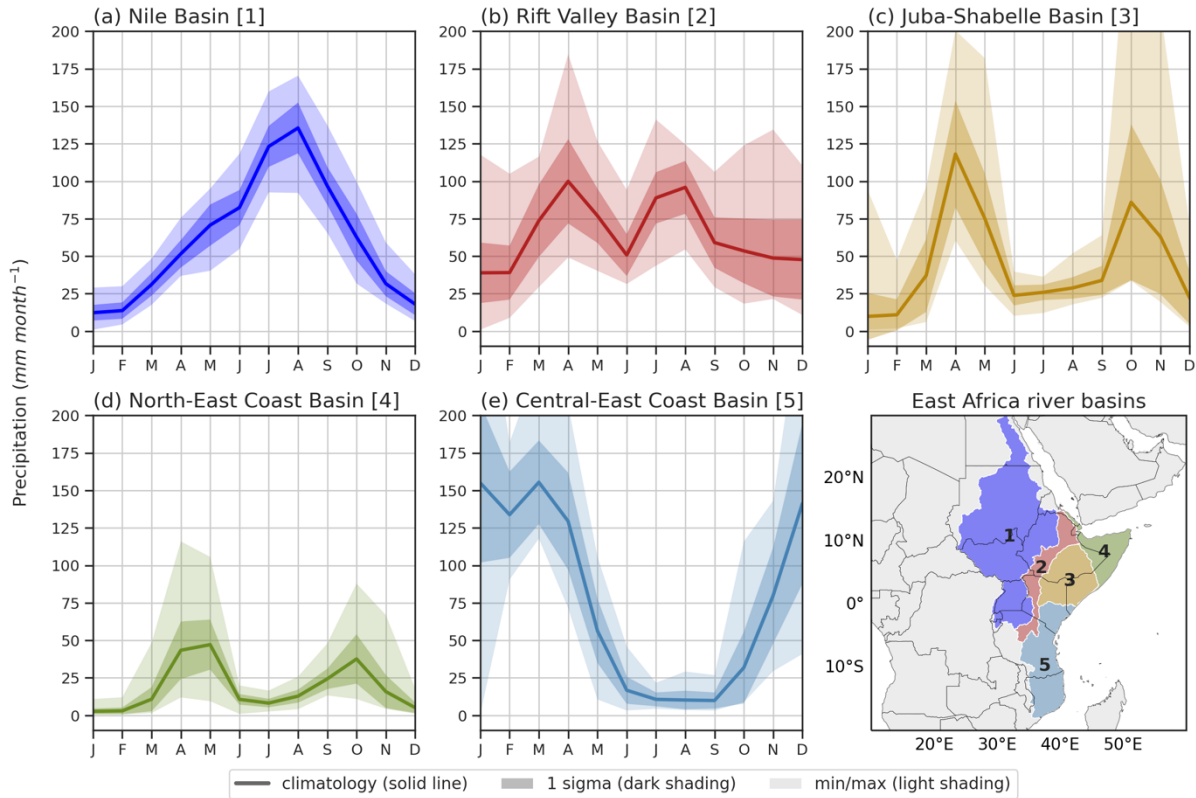


**Figure 1 Seasonal cycle of area-mean rainfall across five river basins (a-e) across Eastern Africa (f), 1983-2019.** **a|** Mean seasonal rainfall in the Nile Basin (area 1 in the map, as delineated by HydroBASINS<sup>254</sup>). The dark blue envelope denotes the standard deviation about the monthly mean values and the light blue envelope the range of values. Values are calculated from the monthly gridded gauge data from the Global Precipitation Climatology Centre (GPCC)<sup>255,256</sup>. **b|** As in a, but for the Rift Valley Basin (area 2 in the map). **c|** As in a, but for the Juba-Shabelle Basin (area 3 in the map). **d|** As in a, but for the North-East Coast Basin (area 4 in the map). **e|** As in a, but for the Central-East Coast Basin (area 5 in the map). Substantial differences in the magnitude, variation and (bimodal) seasonal cycle of rainfall are evident across Eastern Africa.

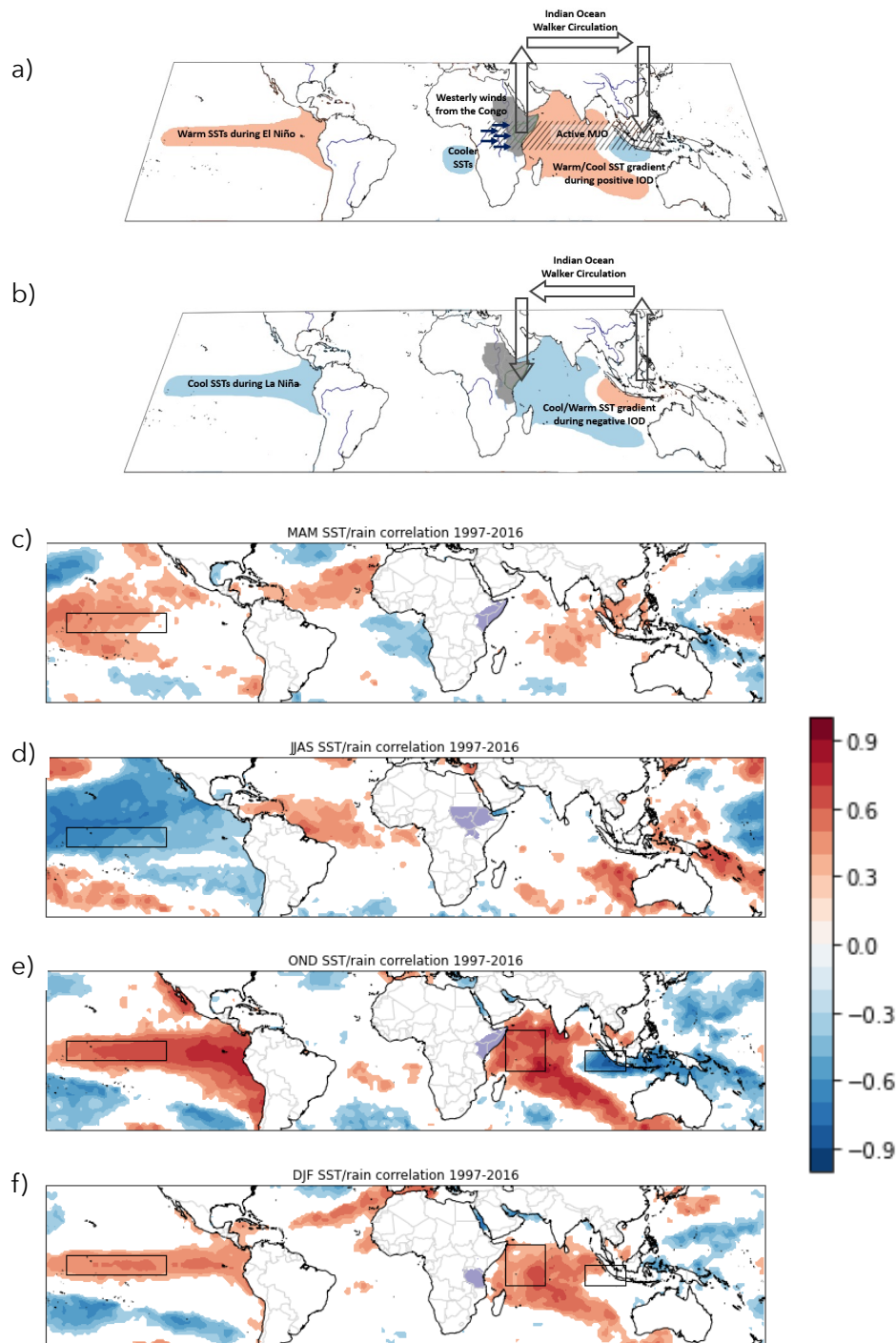


**Figure 2 the main physical processes that determine rainfall variations over Eastern Africa.** **a)** mechanisms that lead to enhanced rainfall over Eastern Africa. Orange and blue shading denotes warm and cool sea surface temperatures (SSTs), respectively **b)** Mechanisms that lead to reduced rainfall over Eastern Africa. Rainfall variations are determined by processes that act on local spatial scales and via atmospheric teleconnections. The green contour marks the region that experiences a bimodal regime. **c-f** seasonal correlations between SST and regional Eastern African rainfall (denoted by areas with purple shading). Black open rectangles over the Pacific and Indian Ocean define the regions we use to calculate the ENSO and IOD.

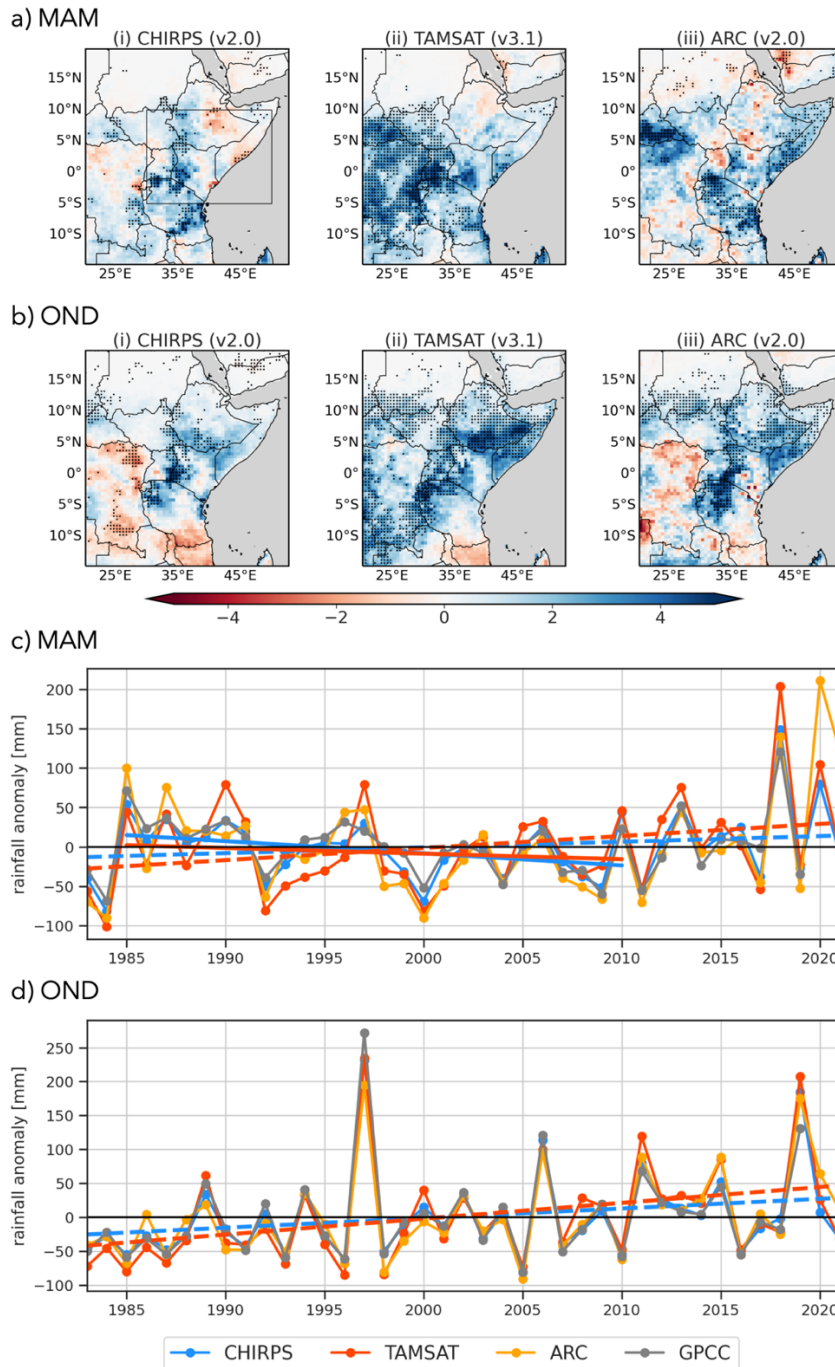


**Figure 3 Spatial and temporal variations of rainfall over Eastern Africa.** **a|** mean rainfall trends during the long rains (MAM) over 1983–2021 for three datasets: CHIRPS<sup>257</sup> (top left); TAMSAT<sup>40</sup> (top middle); and ARC<sup>84</sup> (top right). Stippling denotes statistically significant trends at the 95% confidence level using the Wald test. **b|** as in a, but for the short rain (OND). **c|** area-weighted total rainfall anomalies during MAM over part of Eastern Africa (30–50°E, 5°S–10°N; see box in top left panel of a) for the three datasets, including GPCC. Anomalies are calculated relative to the 1983–2021 monthly means. **d|** As in c, but for OND. Dashed and solid lines denote linear trend lines for CHIRPS and TAMSAT over periods 1983–2021 and 1985–2010, respectively, with colours corresponding to the data; the shorter period is used to highlight changes in the long rains in the 1990s. There is better agreement between trends determined by different rainfall data products for the short rains.

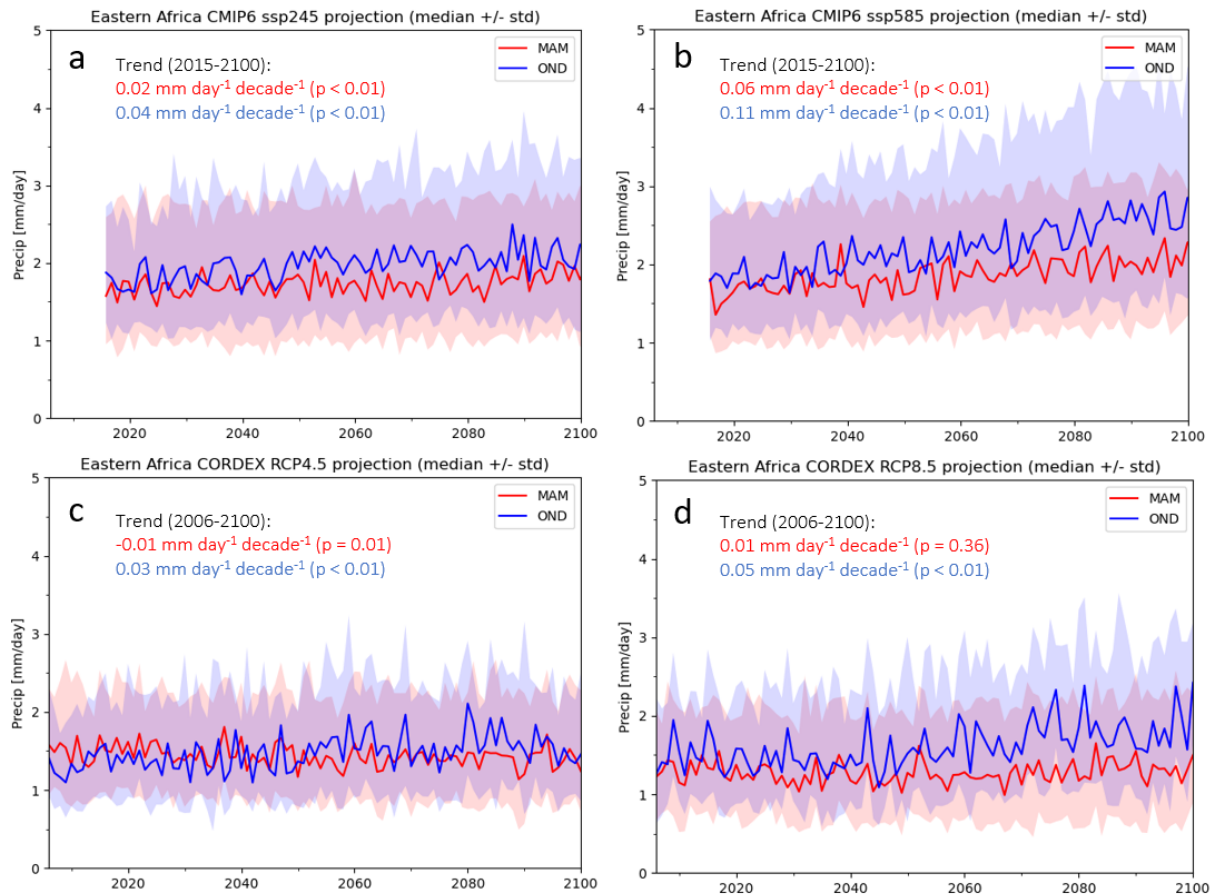


**Figure 4 Projections of long rains and short rains.** **a)** Multi-model median long rain (MAM; red) and short rain (OND; blue) projections from CMIP6 models forced under SSP 2-4.5. Shading denotes the standard deviation associated with the ensemble of model runs. **b)** As in **a**, but for CMIP6 models forced under SSP 5-8.5. **c)** Multi-model median long rain (MAM; red) and short rain (OND; blue) projections from CORDEX regional climate models forced with RCP4.5. **d)** As in **c**, but for CORDEX regional climate forced with RCP8.5. Global and regional climate model projections suggest that short rain totals will exceed those of the long rains, the timing of which depends on the future scenario.

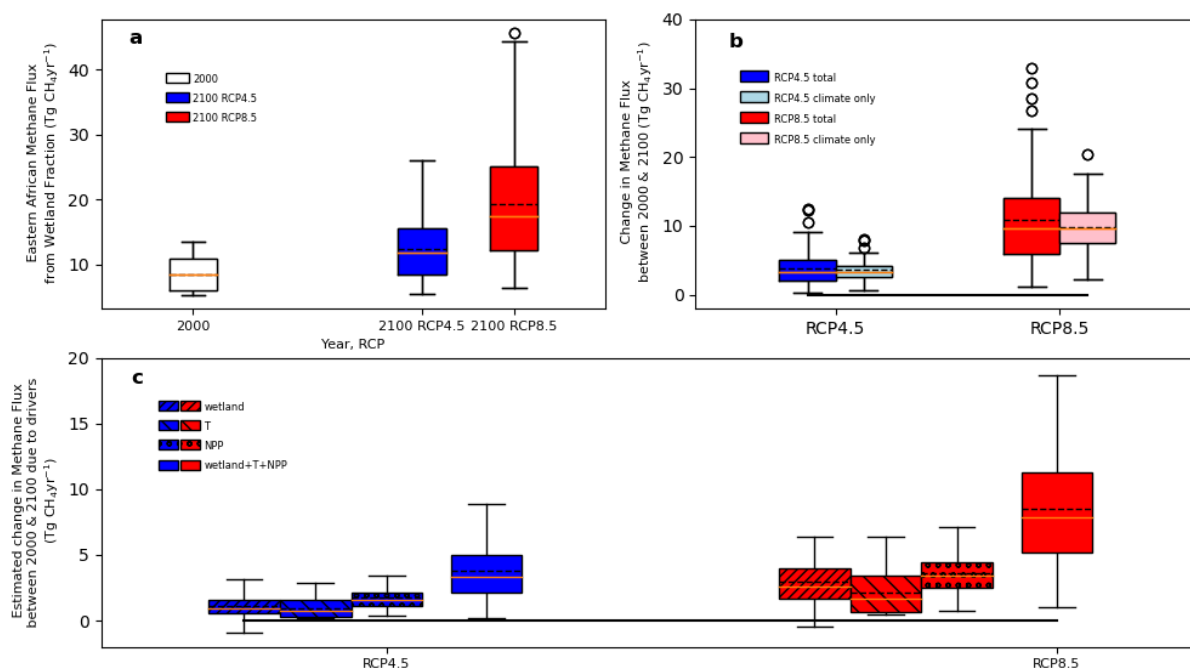


**Figure 5 Wetland methane emission over Eastern Africa.** **a|** methane emission estimates from the JULES model for 2000 (white) and 2100 driven by RCP4.5 (blue) and RCP8.5 (red). **b|** changes in methane emission estimates between 2000 and 2100 for RCP4.5 and RCP8.5. Spread, denoting climate uncertainty, is shown by light blue (RCP4.5) and pink (RCP8.5) box and whiskers. **c|** linearised estimates of changes to methane emissions from 2000 to 2100 under RCP4.5 and RCP8.5<sup>258</sup> owing to inundation extent, soil temperature, NPP and inundation extent + soil temperature + NPP. In all cases, boxes describe the interquartile range (IQR), the whiskers the quartiles  $\pm 1.5 \times \text{IQR}$ , circles outliers, and the orange and dashed black lines the mean and median values, respectively, associated with the ensemble of model runs. Future increases in methane emissions are driven approximately equally by warmer temperature, higher rainfall and larger NPP. The solid horizontal lines in b and c denote the zero line.



## Supplementary Information << new file >>

To understand the response of wetland methane emissions over Eastern Africa to future climate output from the JULES land surface model<sup>259,260</sup> is analysed, coupled with the IMOGEN impacts model<sup>258,261</sup>. IMOGEN is calibrated against 34 different CMIP5 ESM-based climate simulations where the climate is described using pattern-scaling<sup>262</sup>.

Fitted to the climate projection from each ESM, IMOGEN assumes a linear relationship at each grid-box and for each month between changes in meteorology and global warming, itself a function of atmospheric radiative forcing. The IMOGEN system allows an exploration of the uncertainty in the climate projections and the wetland methane emission models. The JULES wetland methane emissions model is driven by wetland extent, available substrate, and soil temperature.

In this analysis net primary productivity as a surrogate for the substrate<sup>258</sup>. Ranges of regional totals are used to described wetland model uncertainty, based on the best current global totals<sup>258</sup> and a range of temperature sensitivities<sup>258</sup>.